AN EXPERIMENTAL STUDY ON THE INFLUENCE OF MISALIGNMENTS ON THE STATIC TRANSMISSION ERROR OF HYPOID GEAR PAIRS

THESIS

Presented in Partial Fulfillment of the Requirements for the Degree Master of Science in the Graduate School of The Ohio State University

By

Sandeep Makam, B.Tech

Graduate Program in Mechanical Engineering

The Ohio State University

2010

Master's Examination Committee:

Professor Ahmet Kahraman, Advisor

Dr. Sandeep Vijayakar

ABSTRACT

An experimental investigation was performed in this study to quantify the influence of gear position errors and misalignments on the loaded static transmission error of a hypoid gear pair. A test machine was designed and procured for this purpose to allow operation of a hypoid gear pair under a given constant torque and at a very low rotational speed. The test set-up incorporated a capability to induce any type of misalignment at any user defined magnitude, including pinion (H), gear (G), shaft off-set (V) and shaft angle (γ) errors, independent of each other in a tightly controlled manner. An encoder-based transmission error measurement system incorporated with the test machine consisted of two high-precision angular optical encoders and a special-purpose analyzer to obtain the transmission error in both time and frequency domains.

The test matrix considered in this study included all four types of misalignments at various magnitudes, drive and coast side conditions as well as a typical range of input torque. A 4.1 ratio hypoid gear pair from an automotive axle application was used as the example system. The test results were presented in the form of the variation of the first three harmonic amplitudes of the transmission error as a function of torque and error magnitudes. It was shown the each misalignment impacts the transmission error in different levels. The drive and coast side transmission error measurements were shown

to differ as well. A nearly “V-shaped” dependence of the first harmonic amplitude of the transmission error to the torque transmitted was also documented regardless of the error type and magnitude applied to the gear pair.

DEDICATION

This document is dedicated to my mom, dad and a friend whose memories I cherish.

ACKNOWLEDGMENTS

I would like to express my sincere gratitude to my advisor, Prof. Ahmet Kahraman, for this great research opportunity, his guidance throughout my research and his effort in reviewing this dissertation. I am really grateful for his support and advise at various stages of my program. I would also like to express my appreciation to Dr. Sandeep Vijayakar for his patience and effort in being a part of my Masters examination committee.

I would like to thank the sponsors of the Gear and Power Transmission Research Laboratory, especially Mazda, Japan and American Axle and Company, Michigan for their financial support throughout my study. I would like to specially thank Samuel Shon for his help, patience and guidance throughout my experiments. I would also like to thank Jonny Harianto and all my lab mates for their help and friendship throughout my study at OSU and beyond.

Finally, I deeply appreciate the love and trust shown toward me by my parents, and grandparents, for all of their support and encouragement. A special mention to Sudeeksha for her unfailing encouragement and patience all through. I would also like to thank all my friends here at Columbus for making my life here very memorable.

VITA

June 2004 ....National Public School, Bangalore, India

2008...B.Tech. Mechanical Engineering, Indian Institute of Technology Madras, Chennai, India

2008 to present ....Graduate Research Associate, Gear and Power Transmission Research Laboratory, Department of Mechanical Engineering, The Ohio State University

FIELDS OF STUDY

Major Field: Mechanical Engineering

TABLE OF CONTENTS

LIST OF TABLES

LIST OF FIGURES

NOMENCLATURE

TE	Transmission Error
H	Pinion position error
V	Shaft off-set error
G	Gear position error
γ	Shaft angle error
θ_p	Angle of rotation of pinion
θ_g	Angle of rotation of gear
N_p	Number of teeth on pinion
N_g	Number of teeth on gear
H_{im}	i^{th} gear mesh order
A_{im}	i^{th} gear mesh harmonic amplitude of the transmission error at H_{im}

CHAPTER 1

INTRODUCTION

1.1 Background, Literature Survey and Motivation

Hypoid gears can be considered as the most general form of gearing in terms of their configuration and geometric features where other forms of gearing can be obtained by assigning certain values to certain geometric parameters. They are designed to transfer power between two non-intersecting cross-axis shafts. These gears find their most extensive and high-volume uses in automotive front and the rear axle units as well as other components such as power-take-off units for auxiliary functions in special vehicles. Spiral bevel gears form a special case for hypoid gears where their axes intersect (no shaft off-set). They are manufactured by using the same hobbing or milling processes as hypoid gears. With this, spiral bevel gears, as used widely in rotorcraft gear drive trains, are also subject to issues associated with hypoid gears. As compared to spiral bevel gears, hypoid gears are stronger, and can achieve higher reduction ratios.

Hypoid gears have complex geometries produced by manufacturing processes that involve a large number of machine setting parameters as well as cutting tool parameters [1]. In addition to the complexity of the manufacturing processes, hypoid gears have other issues that must be dealt with. One such issue is the mechanical power losses experienced at the gear mesh due to higher levels of relative sliding originating from the kinematics of the contact surfaces and the shaft off-set. The other issue involves the locations of the contact along the tooth surfaces that impact both durability and noise characteristics of hypoid gear pairs. The location of the contact patch is highly sensitive to the relative position of the two gears (called pinion and gear in this study) forming the pair with respect to each other. Deviations from the desired nominal position due to mounting errors, housing manufacturing errors and deflections are known to change the contact zone location [1-4]. These deviations, often called *misalignments*, not only influence the contact and tooth root stresses but also the vibration excitations generated at the gear mesh [2-5].

In the gear dynamic field, the motion transmission error of a gear pair, called *the transmission error*, has been widely recognized as one of the measures representing vibration excitations at the gear mesh causing noise. Transmission error of gears can be defined in simple terms as the deviation of the driven gear from its theoretical position defined by the gear ratio [6-10]. It is usually described in terms of a displacement along the line of action for parallel-axis gears and in rotations (relative to input or output) for cross-axis gears. There are several models [3, 4, 11-13] that predict the transmission error of hypoid gear pairs with or without misalignments. There have been additional formulations to theoretically find the location of the contact zone at a given set of errors or determine the error values to result in a particular error position [14]. These prediction models, however, were not validated extensively due to the lack of transmission error data under loaded conditions in the presence of known misalignments conditions.

Various studies on measurement of loaded transmission error in parallel and crossed-axes gear systems have been conducted in the past. These studies can be classified in two groups. One group of studies focused on measurement of transmission error of spur and helical gears under dynamic conditions. As optical encoders are not suitable in such high-speed conditions, tangentially mounted linear accelerometers were used in these studies to measure the dynamic transmission error [15-20]. The other group of measurements used angular encoders to measure the transmission error under low-speed (quasi-static) conditions [21, 22]. In these studies, the signals from the encoders attached to the pinion and gear were compared to each other or to a high-frequency reference signal to predict the transmission error of the gear pair.

At the Ohio State University, a series of investigations starting with Dziech [23] focused on development of a bevel gear static transmission error test stand for performing tests under loaded conditions. This set-up used an encoder-based transmission error measurement system. Poling [24] made several additions to the test stand to improve its measurement capabilities and accuracy. Schmitkons [25] further attempted to improve its results and performance. All of these studies indicated the effectiveness of the encoder method to measure loaded transmission error of a cross-axis gear pair. However, various torque and speed control issues associated with the friction brake were reported to hamper the accuracy of the results. More recently, Gosselin et al [26] conducted loaded transmission error measurements on hypoid gears. The loaded static transmission error of a Formate hypoid gear set was measured within a range applied load using an optical encoder method as well as an analog measurement method. They ran the gears at in input rotational speed of 20 rpm and varied the input torque in steps of 300 Nm up to 900 Nm. Based on limited data included in this paper, they confirmed the previously established fact that transmission error amplitudes change with applied load. This study did not deal with any sort of misalignments and their effect on the transmission error amplitudes.

1.2 Scope and Objective

The above review of the literature points to the lack of an extensive experimental database of loaded transmission error for hypoid gear pairs with various misalignments. Generation of such a database would not only provide much needed data for the validation of the prediction models but also provide an empirical understanding of the combined influence of torque and misalignments on hypoid gear transmission error. Accordingly, this research focuses on development of such a database using a typical hypoid gear pair from an automotive rear axle. As no experimental set-up was available at the start of this activity, this research emphasizes the development of a facility as well as the generation of the database. The specific objectives of this study are as follows:

- Development a test set-up capable of operating a hypoid gear pair up to an input torque of 500 Nm while maintaining a constant low rotational speed. This torque range is representative of the actual application of the gear pairs of interest.
- Development and implementation of mechanisms/schemes to apply and tightly control all four basic types of misalignments in a repeatable manner.
- Devising an angular encoder based system for measuring the transmission error of the gear pair during both drive and coast side operation.
- Defining and implementing a detailed test matrix to form an experimental database, which contains measurements at different misalignment conditions within the entire range of torque.

This study is experimental in nature as modeling and model validation aspects of the problem are beyond the scope of it.

1.3 Thesis Outline

The rest of this thesis is organized in three chapters. Chapter 2 describes the test methodology developed specifically for this study. It describes the hypoid gear test rig and its principal components. The procedures to apply all four types of misalignments, the instrumentation and measurement systems used in data acquisition, the test procedure, test specimens and the test matrix are all described in Chapter 2. Chapter 3 starts with the backlash measurements as well as the results of the repeatability tests. The transmission error measurements with and without misalignments are presented next for both drive and coast side operations. The final chapter summarizes this work, lists its major conclusions and provides a list of recommendations for future work.

CHAPTER 2

HYPOID GEAR TEST METHODOLOGY

2.1 Introduction

This chapter presents the essential details of the hypoid gear test machine developed specifically for the purposes of this project and another companion study on the influence of misalignments on root strains of hypoid gears [5]. Main components of the test set-up (torque-motor, torque-meter, optical encoders, spindles holding gears, magnetic particle brake and the torque reducing belt drive), measurement systems, error application schemes as well as data analysis system are discussed. Readers are referred to Hotait [5] for further details.

In this chapter, unique mechanical features of the test set-up will be described first. The instrumentation and measurement systems used in data acquisition will be presented and the test procedure will be described in detail. The methods developed to intentionally misalign the gears in various directions will be described next. The chapter ends with details about the example hypoid gears and a detailed test matrix for conducting the experiments, the results of which are reported further in Chapter 3.

2.2 Description of the Hypoid Gear Pair Test Machine

The machine used in this study to measure the loaded static transmission error of a pair of hypoid gears is shown in Figure 1. It consists of two high precision spindles, a torque-motor, a torque-meter, a universal joint, a magnetic particle brake, a torque-reducing belt drive, and two high-precision optical encoders along with a pair of hypoid gear pairs, as labeled in the top-view schematic layout, of Figure 2.

As the goal here is to measure transmission error (TE) of the hypoid gear pair under loaded but quasi-static conditions, a DC torque-motor (Sierracin Magnedyne, 491-10) that can deliver torques up to 1350 Nm (12,000 lb-in) at speeds up to 15 rpm is used. This special-purpose torque-motor has seven pairs of brushes, 28 poles and 253 commutator bars designed to generate such torque levels at very low speeds. These very low speed conditions ensure that no dynamic (vibratory) effects are present to influence the measurements.

A shown in Figure 2, a torque-sensor (Lebow, 1228-10K) is connected to the shaft of the torque-motor to measure the torque provided to the hypoid pinion for not only monitoring the torque input, but also controlling it through feedback to the

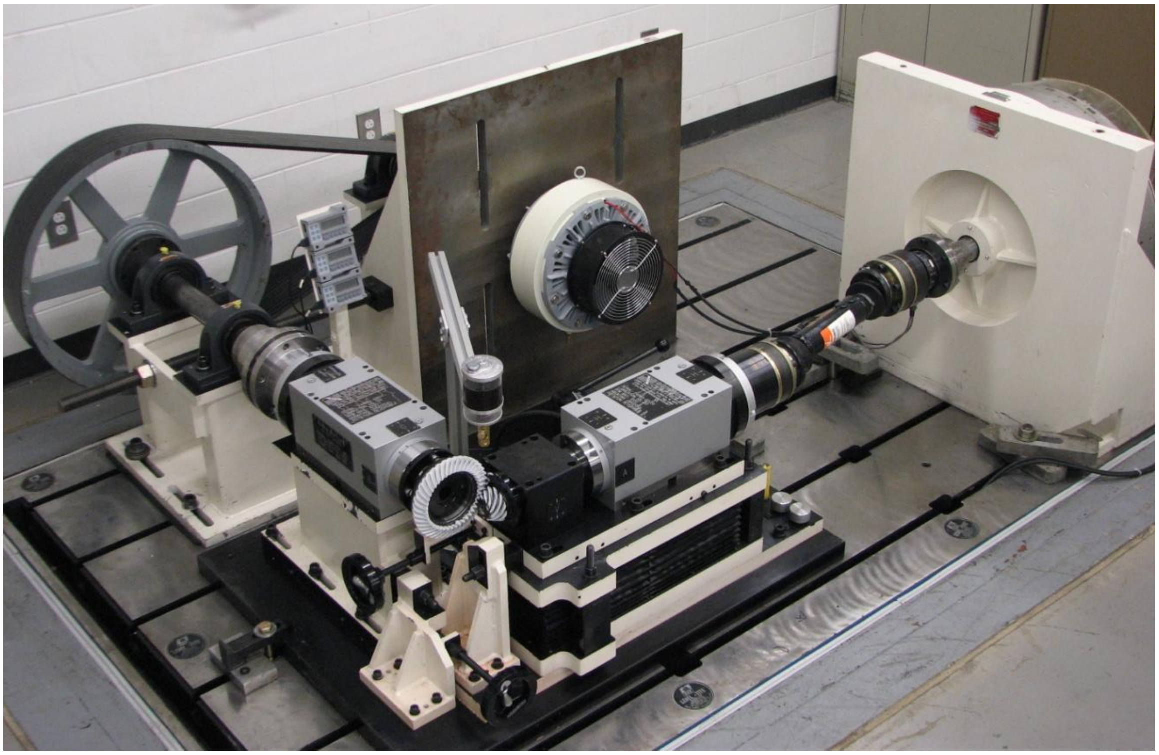

Figure 1: Picture of the hypoid gear test machine used in this study.

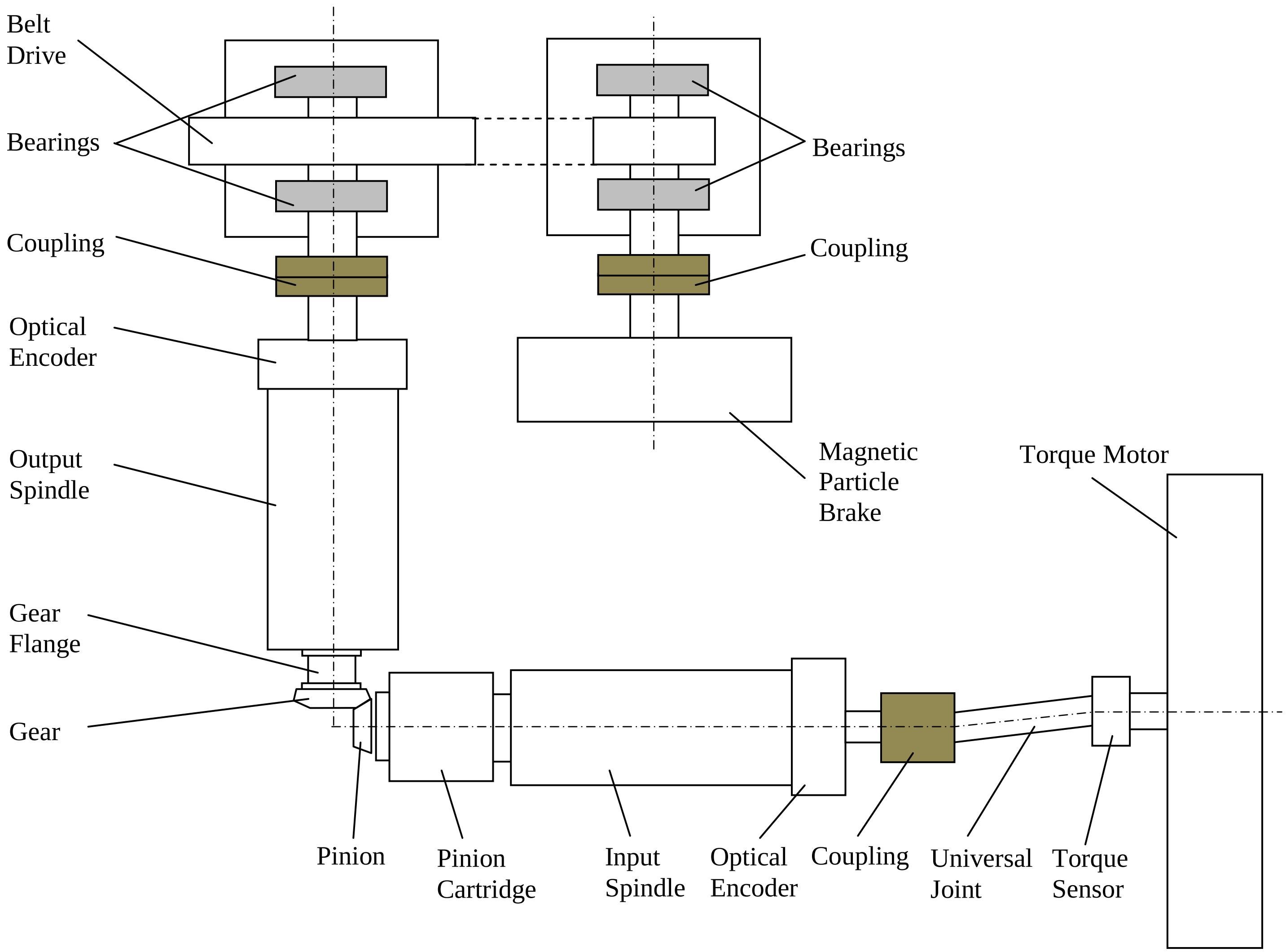

Figure 2: Top view schematic layout of the hypoid gear test machine showing its main components.

machine's PLC controller. The Lebow torque-sensor has a maximum working torque range of 1130 Nm (10,000 lb-in).

Also shown in Figure 2 is a rigid, high-precision input spindle that was designed to hold and allow rotation of the pinion at desired positions under load. In addition, it holds a precision optical encoder to measure the angular position of the pinion. At the other end, the input spindle is connected to the pinion that is held by a rigid cartridge. The cartridge is designed to hold the pinion exactly the same way as in the axle assembly using the production pinions. Figure 3(b) shows a cross-section of this pinion cartridge assembly with its pinion and bearings. Design of this pinion cartridge was specific to the gear pair to be tested. The advantage of this arrangement is that the machine can be used to test other sizes of hypoid or spiral bevel gear sets by simply changing the pinion cartridge and minor details of the flange holding the gear. This cartridge design also allows for pinion bearings to be preloaded axially, exactly the same way in the actual product.

On the gear axis side of the layout shown in Figure 2, the hypoid gear is held by a custom-made flange the same exact way the gear is attached to the differential assembly in the actual product. Cross-sectional detail of this holding method is shown in Figure 3(a). Again, a different hypoid gear design would require this flange to be modified. Another rigid, high-precision spindle holds the gear flange as well as another optical encoder on the other side.

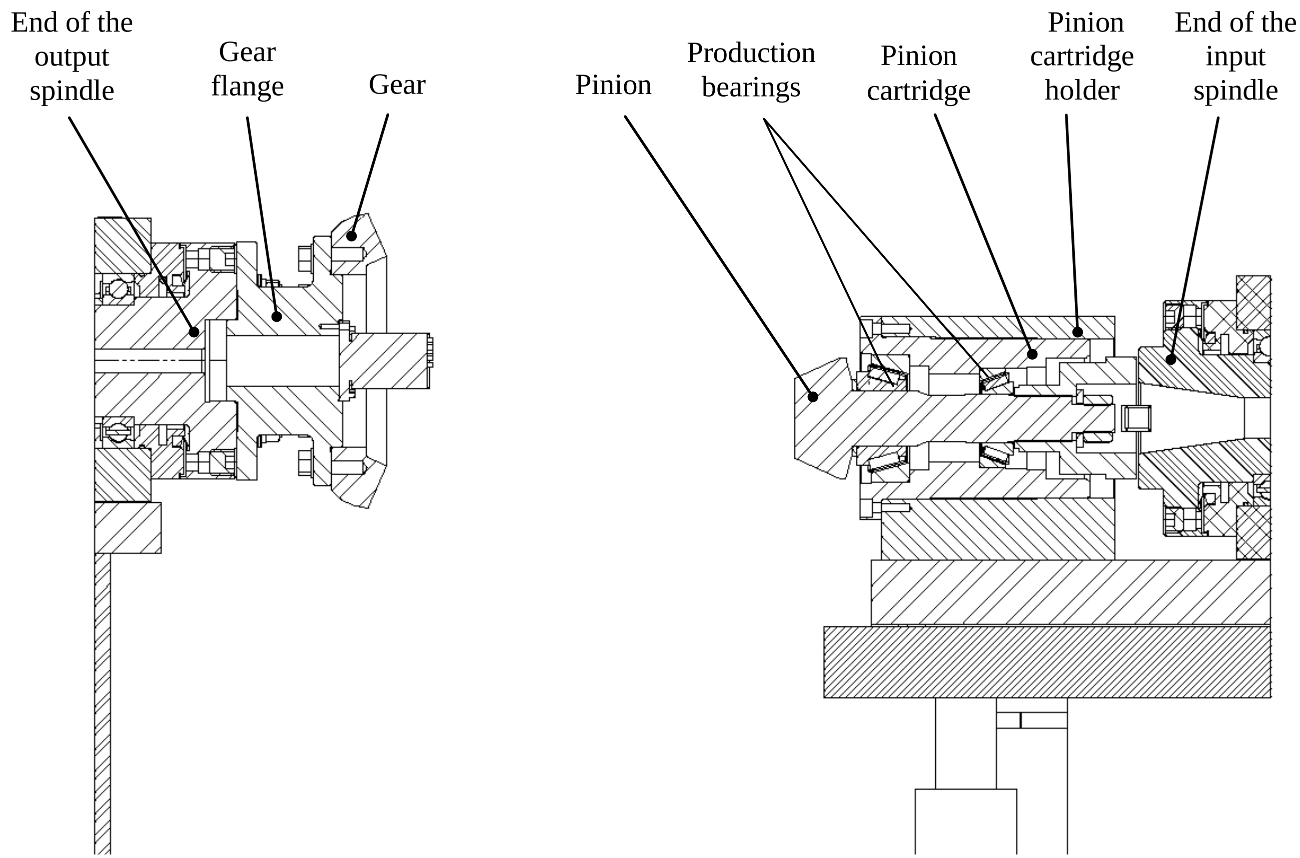

(a) (b)

Figure 3: Mounting details of Rear Axle gear pair.

Since speed ratios in excess of 4:1 are typical for hypoid gear sets of rear axles, the torque values on the output side can be more than four times the input torque. This would require a very high torque capacity brake that must operate at speeds less than 4 rpm. Such a brake would be very large and costly. For this reason, the output spindle was connected to a 1:5 belt drive to act as a speed increaser (torque reducer) as shown in Figure 2. This way, a much smaller brake connected to the high speed pulley of the belt drive would be sufficient to provide desired levels of reaction (output) torque.

A Placid Industries magnetic particle brake was used to apply the load to the test stand. The PFB 400 brake has a ±2% cycle-to-cycle accuracy and is rated to a maximum load of 500 Nm. With a 4:1 ratio gear pair, this allows tests up to 625 Nm input torque. When the brake is not powered, the input is free to turn with the shaft to some minimum amount of drag.

2.3 Instrumentation and Measurement Systems

The TE measurement system was designed for processing the signals from two precision angular encoders shown in Figures 1 and 2. Here, the encoders were connected to the input and output spindles at the opposite ends from the gear and the pinion. As the torsional stiffnesses of spindles were very high, measured angular positions at these encoder locations represented the gear and pinion positions.

Both encoders were identical. They were high-end precision encoders (Heidenhain, RON886) with 36,000 lines per revolution. They had an angular resolution of 0.9 μrad, which is more than sufficient for this application. As shown schematically in Figure 4, the encoder signals were first conditioned using Heidenhain encoder conditioners (IBV600). The output from one conditioner was fed into another conditioner to split the signal. One of the split outputs and the signal from the other encoder were fed into a state-of-the-art transmission error analysis system (Superior Controls, Inc. Transmission Error Measurement System, TEMS) for processing of the data that was displayed on a PC. The standard outputs from the software application of TEMS include the measured raw time domain TE signals (relative to input and output) as well as the processed data (short term (low-pass filtered) TE, long term (high-pass filtered) TE and TE frequency spectrum).

Here, the TEMS software gives the option to computed the transmission error with respect to the input or output rotation. These two forms of TE are defined mathematically as:

$$TE_{out}(t) = \theta_g(t) - \frac{N_p}{N_g}\theta_p(t)\,, \tag{1a}$$

$$TE_{in}(t) = \frac{N_g}{N_p}\theta_g(t) - \theta_p(t)\,, \tag{1b}$$

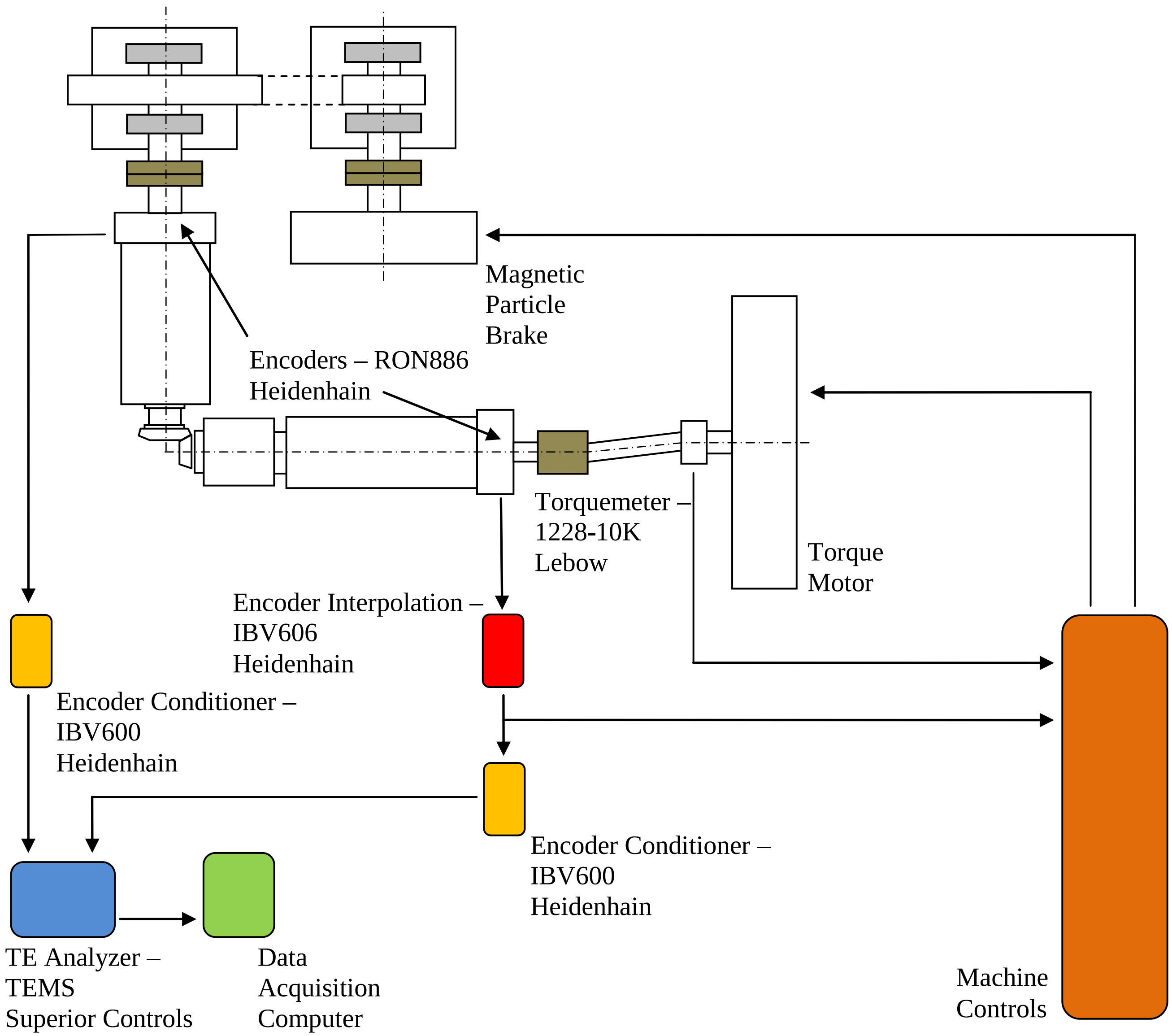

Figure 4: Schematic showing the control-setup and the data acquisition system in the hypoid test rig.

where $\theta_p(t)$ and $\theta_g(t)$ are pinion and gear rotational positions in μrad, N_p and N_g are the number of teeth of the pinion and gear and $TE_{in}(t)$ and $TE_{out}(t)$ are the input and output-based TE values in μrad. From Eq. (1a) and (b), it can be stated that $TE_{in}(t) = \frac{N_g}{N_p} TE_{out}(t)$ theoretically. However, computation of $TE_{in}(t)$ and $TE_{out}(t)$ in TEMS are not done simultaneously, but rather done by using two sets of data taken one after the other since one encoder signal must be used as the reference signal in real time. Therefore in these measurements, this theoretical relation holds approximately, i.e. $TE_{in}(t) \approx \frac{N_g}{N_p} TE_{out}(t)$. In this arrangement, the frequency spectrum of $TE_{in}(t)$ has the fundamental gear mesh order at N_p while the gear mesh order is at N_g for the frequency spectrum of $TE_{out}(t)$.

2.4 Application of Intentional Misalignments to the Hypoid Gear Pair

As stated in Chapter 1, the main goal of this study was to investigate the impact of position errors on the transmission error. Therefore, special attention was given to the application of tightly-controlled amounts of gear position error (often called alignment errors or simply *misalignments* in the gearing community). There are four basic types of misalignments that can define the positions of the hypoid gears completely. These four misalignments as illustrated in Figure 5, are as follows:

(i) The H error: This error defines deviation of the position of the pinion in axial direction from its nominal location. This error is also called the P error in the gear literature. The positive direction for the H error is when the pinion moves away from the gear.

(ii) The V error: As shown in Figure 5, this error specifies the change in the shaft off-set. An increase in shaft off-set by lowering the pinion or elevating the gear vertically is defined as a positive V error. This error is also referred to as the E error in certain gear publications.

(iii) The G error: This error defines the deviation of the position of the gear from its nominal in the direction of its axis. Here, a positive G error represent increased backlash as gear moves away from the pinion.

(iv) The γ error: This error defines the deviation of the shaft angle from its nominal position as shown in Figure 5. For a hypoid gear, a negative shaft error represents an acute shaft angle while a positive γ means a slightly obtuse shaft angle.

The test machine shown in Figure 1 was equipped with a novel capability to set-up a gear pair at any user defined combination of these four errors. In other words, the

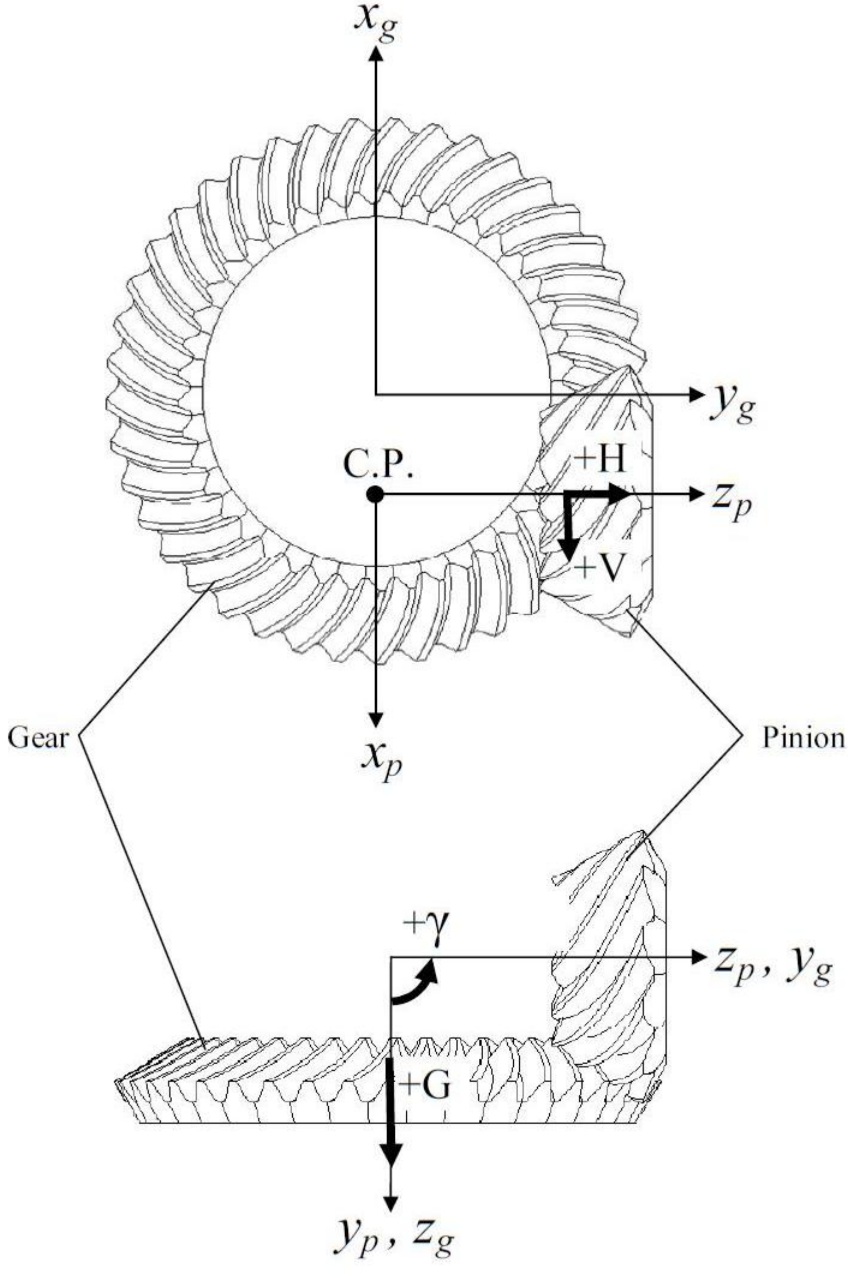

Figure 5: Definition of pinion and gear position errors of a hypoid gear pair.

test set-up was designed to function like a four-axis machine tool. More importantly, it was designed to maintain these set positions under heavily loaded conditions.

2.4.1 Application of the *H* Error

The pinion spindle shown in Figure 6 sits on a slide to allow it to be moved horizontally in the direction of its axis back and forth as defined by the arrow. For this, a set of input spindle bolts clamping the spindle to its table are loosened and the locking bolt on the side is removed to allow an ACME thread jack type positioning device to move the table away from the rigid stop mounted on the base. A calibrated precision kiss block of a desired thickness is placed between the rigid stop and the pinion spindle assembly. The locking bolt is tightened as well as the set of bolts to lock the pinion spindle (hence the pinion) in this horizontal position. Here, one kiss block (*H* block) of a specific thickness represented the nominal position of the pinion at $H = 0$. By producing other blocks with thicknesses at $H = \pm 0.1$ and ± 0.2 mm from this reference gage thickness, different fixed *H* values were obtained. Figure 7 shows a set of five *H* blocks procured for this study. This way, by using different *H* blocks from the set of five in the machine to define the horizontal position of the pinion, discrete error values of $H = -0.2, -0.1,$ 0, 0.1 and 0.2 were possible to achieve.

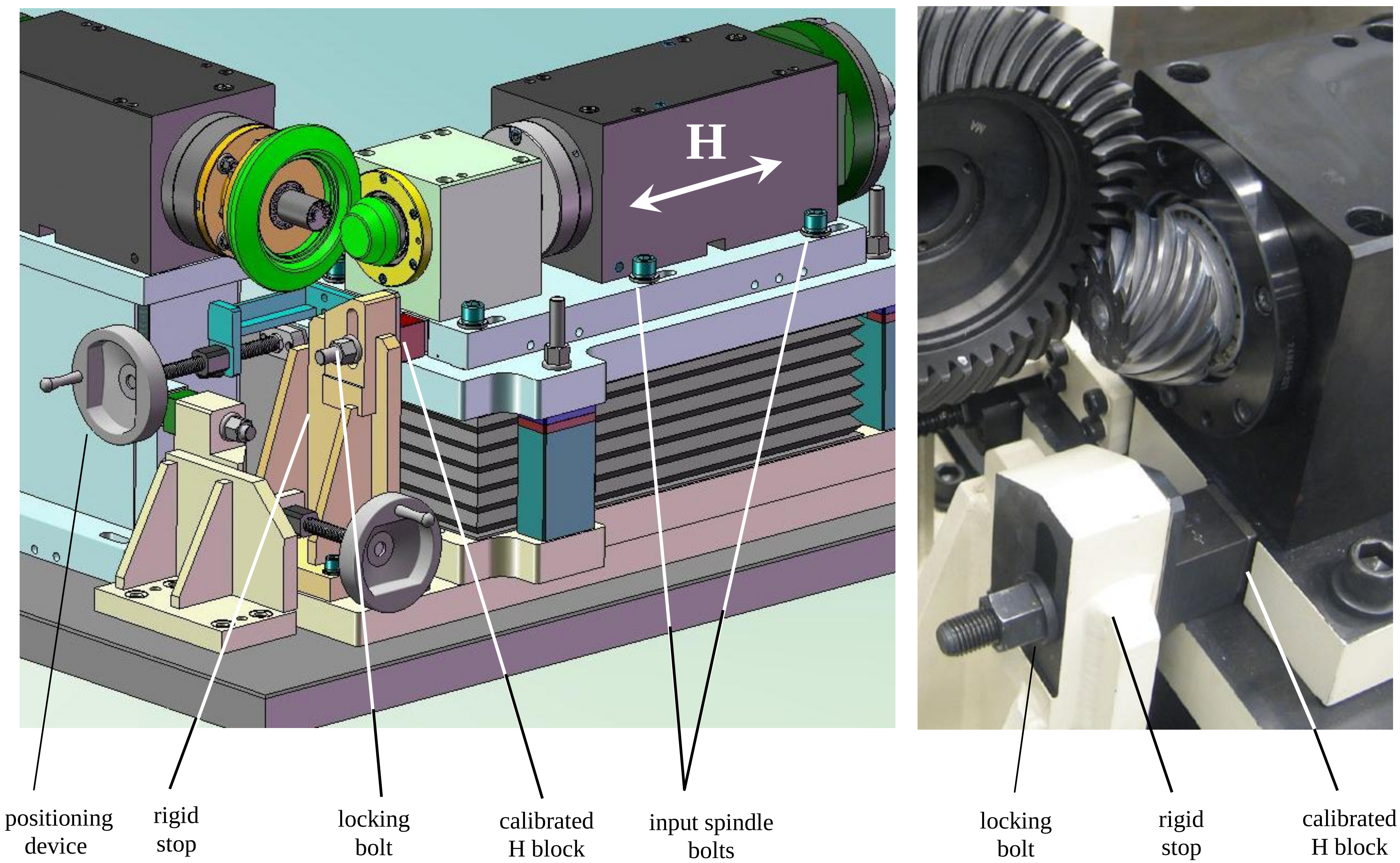

Figure 6: The *H* error set-up mechanism.

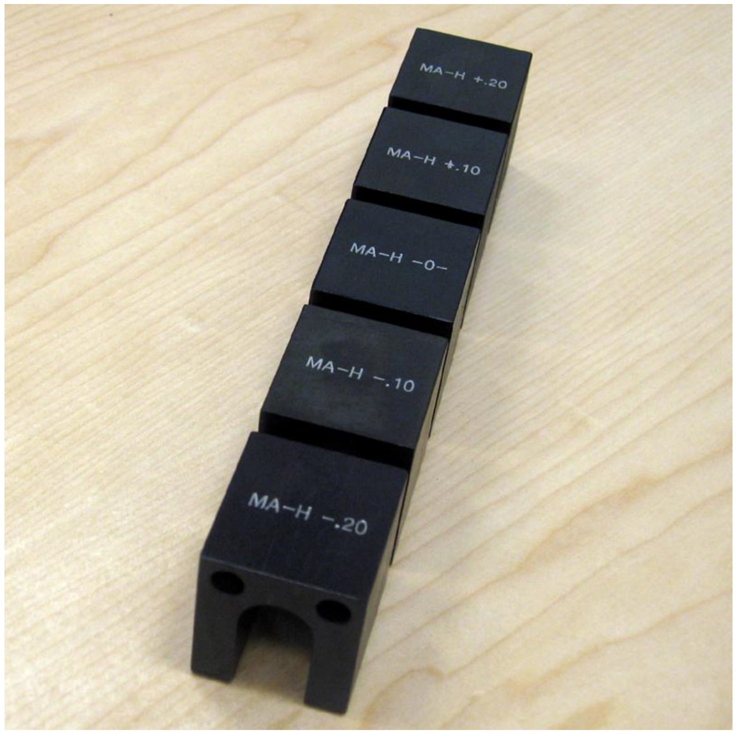

Figure 7: Calibrated *H* blocks.

2.4.2 Application of the *V* error

The adjustment of the vertical position of the pinion relative to the gear (i.e. shaft off-set error *V*) requires the pinion spindle height to be changed. The base of the pinion spindle sits on three rigid legs of equal length. By loosening three locking bolts that fix the spindle base to the base of the machine at these legs and lifting it with a single hydraulic cylinder, a set of three *V* blocks can be placed vertically between the spindle base and the machine base as shown in Figure 8. The blocks forming one of these sets are such that the set shaft offset is equal to the nominal offset. In addition to these no error *V* blocks, other calibrated gauge blocks at different thicknesses were also procured as shown in Figure 9, such that discrete error values of $V = -0.2, -0.1, 0$, 0.1 and 0.2 mm can be achieved for the example hypoid gear pair considered in this study.

2.4.3 Application of the *G* error

Figure 10 illustrates the way the position of the gear is varied in the horizontal direction to induce a *G* error of a given value. The concept here is identical to the one used for setting the *H* error. The spindle holding the gear sits on a table that is allowed to slide on the base in the direction parallel to the axis of the gear. By loosening a set of bolts that fasten the table to the base and removing the locking bolt on the side, the table

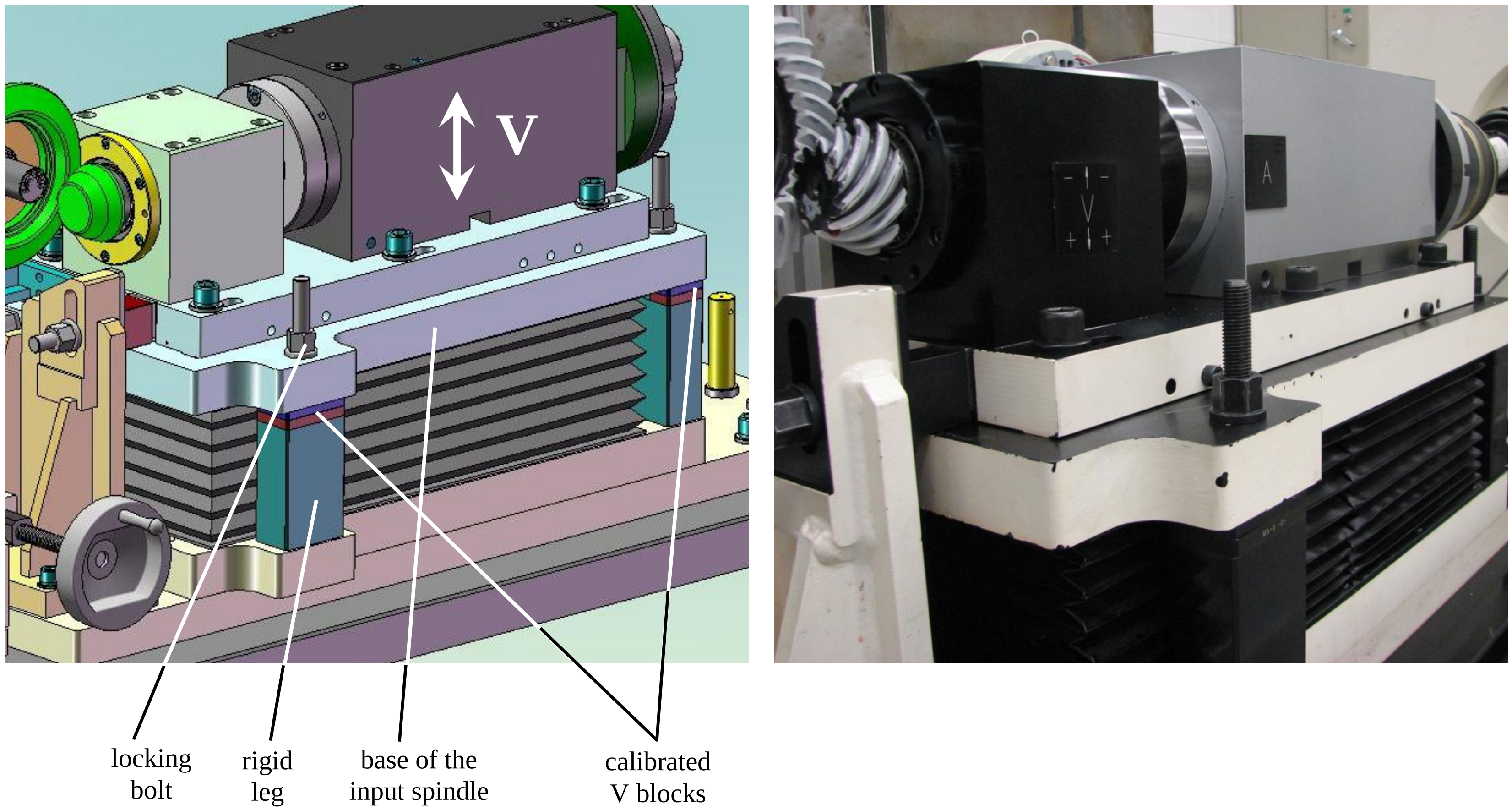

Figure 8: The *V* error set up.

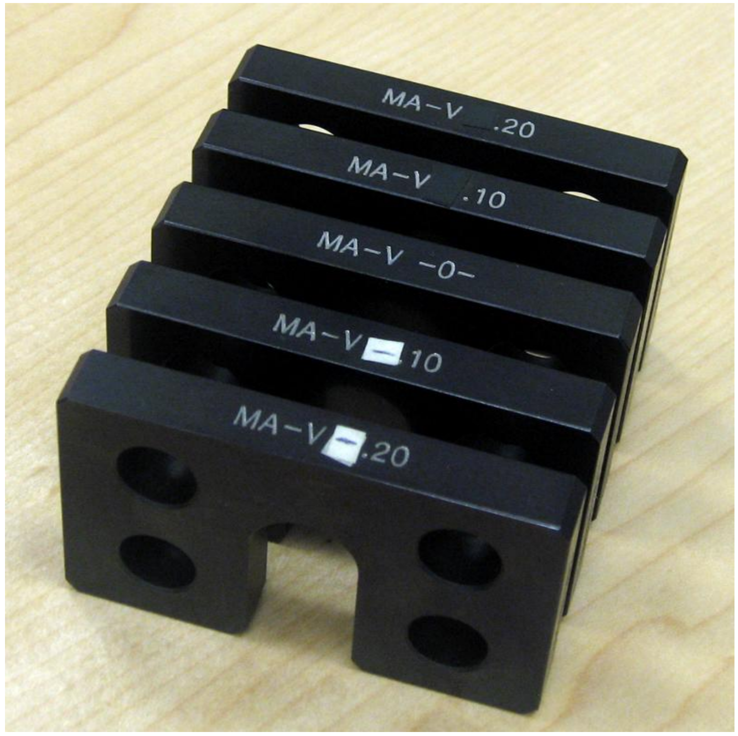

Figure 9: Calibrated *V* blocks.

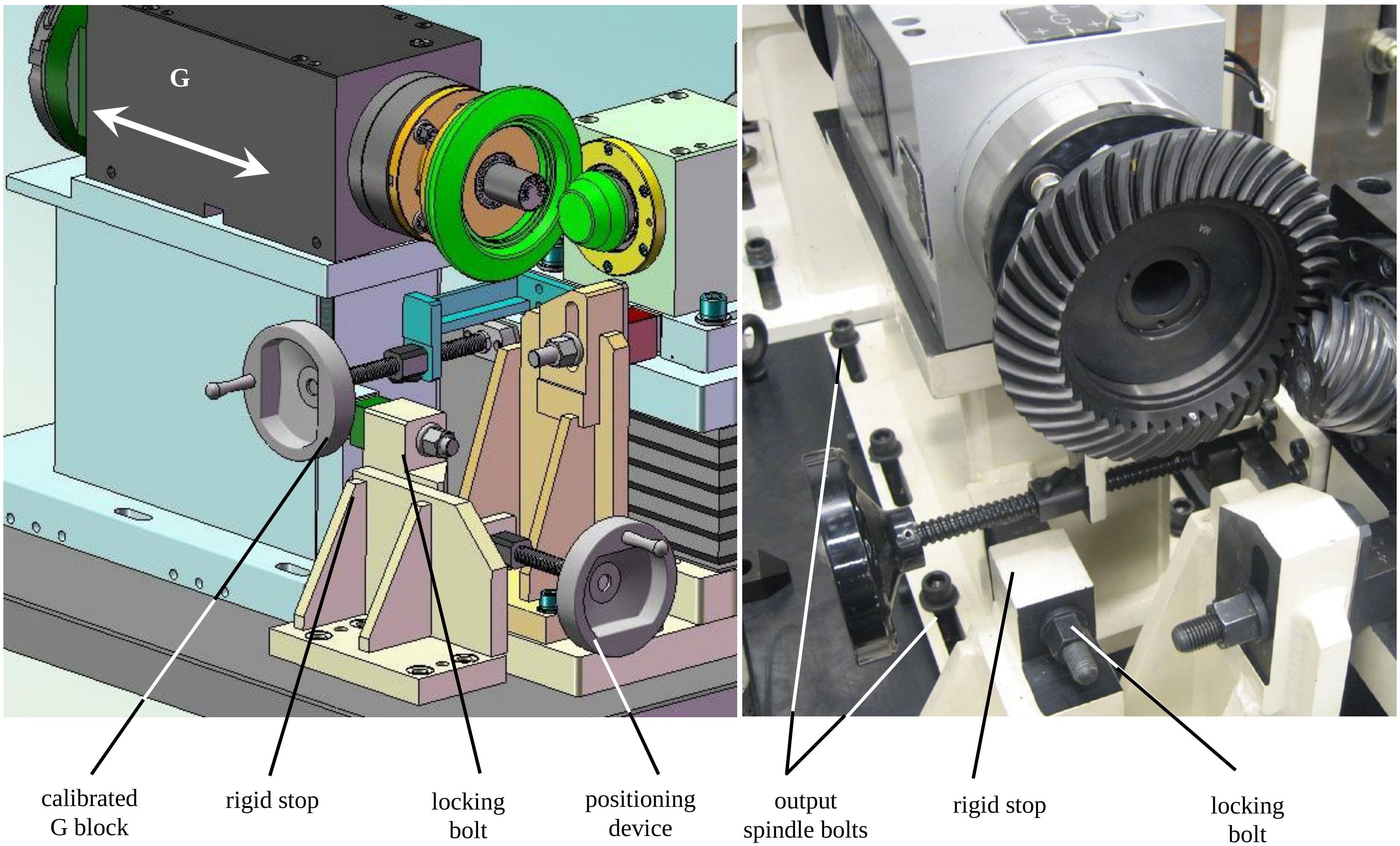

Figure 10: The *G* error set up.

is moved away from the rigid stop mounted on the base using an ACME thread jack type positioning device. A kiss block of certain thickness is used to position the gear horizontally such that $G = 0$. The G blocks of other thicknesses were procured as shown in Figure 11 to achieve discrete error values of $G = -0.05$, 0, 0.1, 0.2 and 0.3 mm in line with the intended application of the example hypoid gear pair.

2.4.4 Application of the γ error

The adjustment to vary the angle between the two shafts from the nominal 90° position ($\gamma = 0^\circ$) requires the pinion to be rotated about its cone apex relative to the gear (or the machine base). The entire assembly consisting of pinion spindle, the pinion spindle base and the three legged machine base is pivoted at the point of projection of the pinion cone apex onto the base as shown in Figure 12. Once the bolts fixing this assembly onto the base of the machine are loosened, this assembly holding the pinion can be rotated freely about its pivot. To rotate the whole assembly, pressurized air is pumped between the moving surfaces to greatly reduce the friction such the whole assembly can be moved easily. By matching a particular pair of dowel pin holes and placing the pin in that location, a certain γ value is achieved. In Figure 12, five such dowel pin holes are implemented to obtain $\gamma = -0.2^\circ, -0.1^\circ, 0^\circ, 0.1^\circ$ and 0.2°, corresponding to the shaft angles of $89.8^\circ, 89.9^\circ, 90^\circ$, 90.1° and 90.2°, respectively.

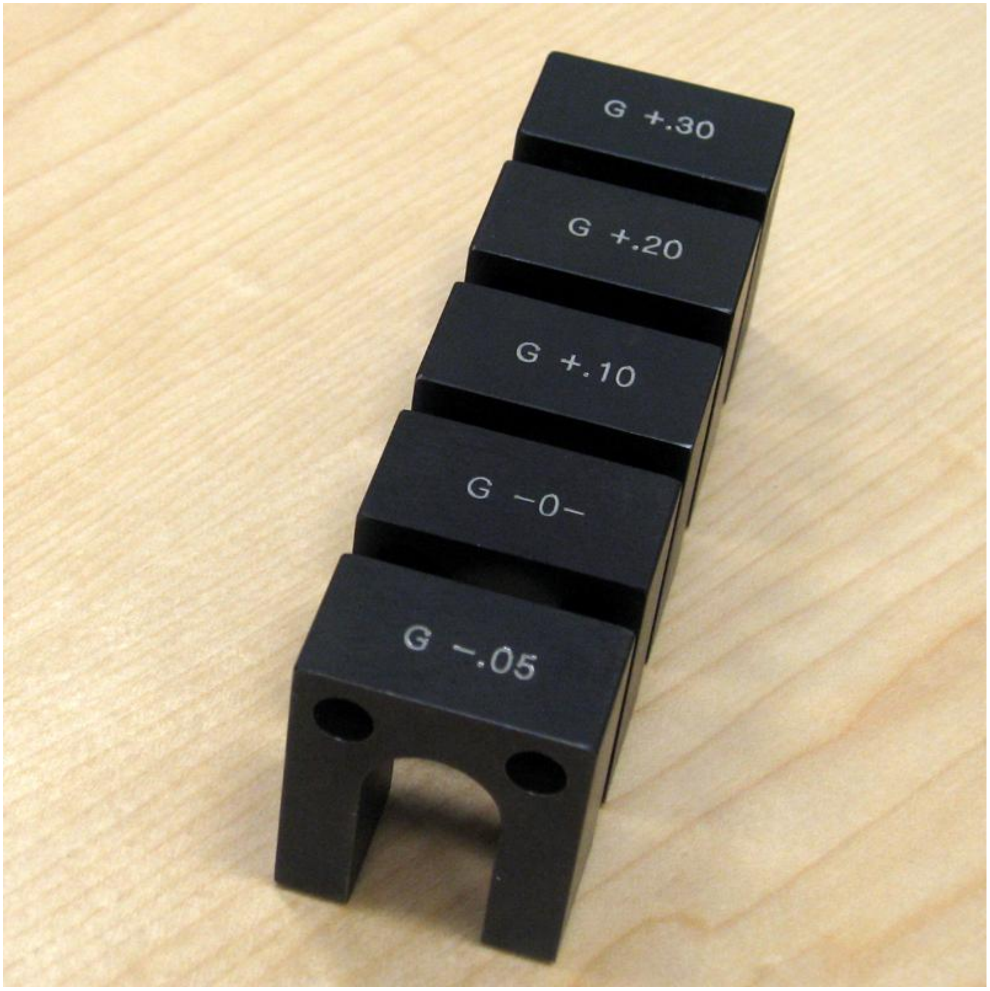

Figure 11: Calibrated *G* blocks.

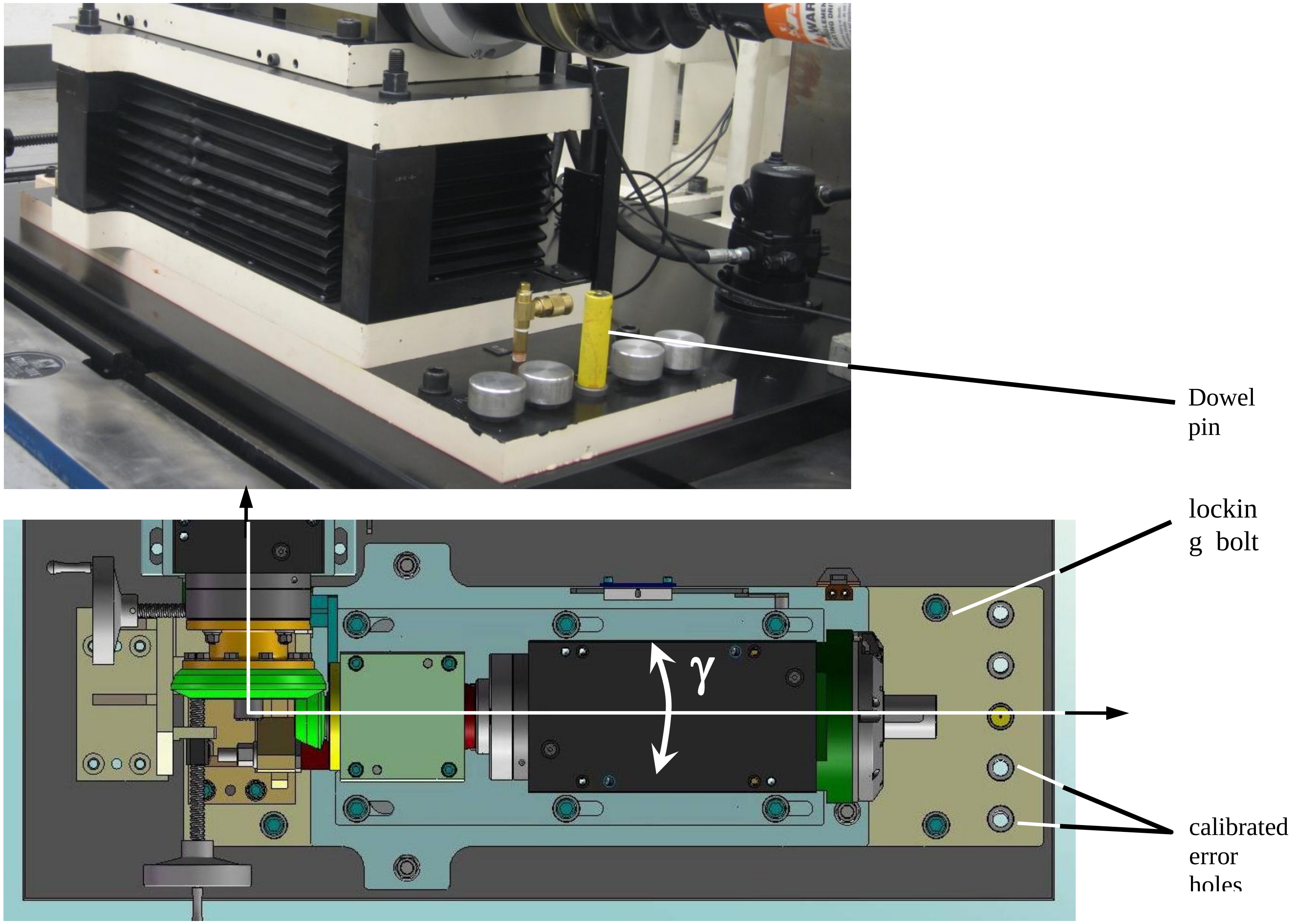

Figure 12: The shaft angle (γ) error set up.

2.5 Test Procedure

Before any TE measurement can be done, desired misalignments must be set up using the capabilities of the machine described above. First step in the test procedure was to use gages corresponding to no error ($V=0$, $H=0$, $G=0$) in addition to place the dowel pin in the middle hole such that $\gamma=0^\circ$. This represents the baseline nominal positions of the gears in relation to each other. Due to the manufacturing errors associated with the gear teeth and blanks, this nominal position often fails to provide the required design backlash value of the gear set. In production axles, the gear is shimmed axially to move it into or away from the pinion to set the backlash value to this desired amount. In order to simulate the same conditions, backlash value of the gear set was measured by using a dial indicator when the gears were at the baseline position. For this, the pinion was held stationary and gear was moved back-and-forth within the backlash region and the resultant circumferential displacement at a point in the middle of the tooth of the gear was measured as the backlash value. Additional gage blocks were added to the *G* block until the backlash value was 0.1 mm that was the design value for this gear pair. In this position, *G* error was called to be zero, i.e. the gear position corresponding to set backlash values. Deviations from the *G* position were then achieved by simply changing the *G* blocks shown in Figure 10 while keeping these additional gage blocks in place.

For the tests with other error combinations, the same reference *G* position was maintained. The effective backlash values of each error combination were measured and any particular error combination that resulted in zero backlash (tight mesh conditions) were eliminated from the test matrix.

An ad-hoc lubrication system was devised that allowed oil drip into the mesh about 6 times a minute. As the gears rotate a very low speeds, this was found to be sufficient to minimize any adverse dry contact conditions.

Next, the gear pair was operated at input speeds of 15 rpm (drive side testing) and –15 rpm (coast side testing) at input torque levels of 0, 200 and 500 Nm load for a few minutes each ensure that the set-up and the controller work properly before starting an actual test. Each test included two individual tests, first a test consisting of 16 rotations of the pinion to compute the TE in terms of input orders using Eq. (1a) and then another test consisting of 16 complete rotations of the gear to compute the TE in terms of the output orders according to Eq. (1b).

For each test, TE data was acquired and stored on a PC via TEMS Software from Superior Controls. The first three output mesh harmonics (integer multiples of the gear mesh frequency) were recorded on a spreadsheet for further analysis and display.

2.6 Test Specimens and Test Matrix

The loaded static transmission error experiments were conducted by using the gears from a small automotive axle unit. The gear pair shown in Figures 1,6,8 and 10, consisted of a 10-tooth pinion and a 41-tooth gear operated at a nominal shaft off-set of 35 mm. Both gears were face-hobbed and then lapped as a pair. Table 1 lists the basic design parameters of the example hypoid gear pair.

Tests were done by loading the gear both under drive and coast conditions. In drive conditions, both input torque and speed were in clockwise direction as viewed from input side (looking at the pinion axially). Opposite load and speed directions were used to obtain the coast conditions. For the baseline no error tests, 20 discrete torque values from unloaded to 500 Nm input pinion torque were considered for both drive and coast side tests. Meanwhile, the tests at a given error value used the input torque values of 0, 100, 200, 300, 400 and 500 Nm. With this, the test matrix shown in Table 2 consisted of 232 individual tests. The results of these tests will be presented and discussed in Chapter 3.

In this research several other test gear pairs of same design having different lapping parameters were also tested as well as a low-ratio hypoid gear set from an automotive power take-off unit. The results of those tests were excluded from this thesis as they were deemed confidential by the sponsor.

Parameters	**Units**	**Pinion**	**Gear**
Number of Teeth		10	41
Hand of Spiral		Left	Right
Mean Spiral Angle	[degree]	52	27
Shaft Angle	[degree]	90	
Shaft Offset	[mm]	35	
Outer Cone Distance	[mm]	93.34	102.18
Outer Diameter	[mm]	80.75	187.65
Face Width	[mm]	37.81	31.00
Cutting Method		Face Hobbed	

Table 1: Basic gear geometry parameters of the test specimens.

Side	**Error Type**	**Error Values** [mm or deg]	**Torque Range** [Nm]	**# of Torque Levels**
Drive	No Error	--	0-500	20
	H	±0.1, ±0.2		6
	G	-0.05, 0.1, 0.2, 0.3		6
	V	±0.1, ±0.2		6
	γ	±0.1, ±0.2		6
Coast	No Error	--	0-500	20
	H	±0.1, ±0.2		6
	G	-0.05, 0.1, 0.2, 0.3		6
	V	±0.1, ±0.2		6
	γ	±0.1, ±0.2		6

Table 2: Test matrix for the loaded static transmission error tests on the hypoid gear pair.

CHAPTER 3

EXPERIMENTAL RESULTS

3.1 Introduction

This chapter presents results of the loaded transmission error tests performed by using the example hypoid gear pair of Table 1, as described in Chapter 2. The data processing procedure will be illustrated first through analysis of an example data segment. Results of a repeatability study will be presented next to demonstrate the combined capability of the test machine and the measurement system in terms of its repeatability. The procedure devised to measure the backlash value of the gear pair at any given error combination will then be introduced and backlash values at each error condition will be listed. The rest of the chapter presents the transmission error measurements conducted on the gear set under both drive and coast conditions. For each operation, as described in the test matrix of Table 2, transmission error is first measured in the nominal error positions under and then each position error is introduced individually to quantify their impact on the transmission error harmonic amplitudes of the transmission error of the gear pair. Discussion of how the torque transmitted and each of the position errors influence the transmission error of the example gear pair under for both drive and coast conditions are presented subsequently.

The actual test matrix considered in this investigation was far more extensive than the one shown in Table 2. It included five pairs of the gear pair design specified in Table 2, each representing different lapping parameters. It also included another set of lower ratio gear pairs from a power take-off unit, again with certain lapping process variations. Results from these additional measurements were not included here since the details of the lapping process parameters were confidential. It can be, however, stated that the same qualitative behavior presented in the following sections for the example hypoid gear pair in terms of the influence of torque and the position errors was exhibited by the other gear pairs as well.

3.2 Analysis of an Example Measurement.

In accordance with the test matrix specified in Table 2, the unfiltered transmission error data at each torque value was recorded with respect to output and input rotations as shown in Figures 13(a) and (b), respectively. These $TE_{out}(t)$ and $TE_{in}(t)$ time histories as

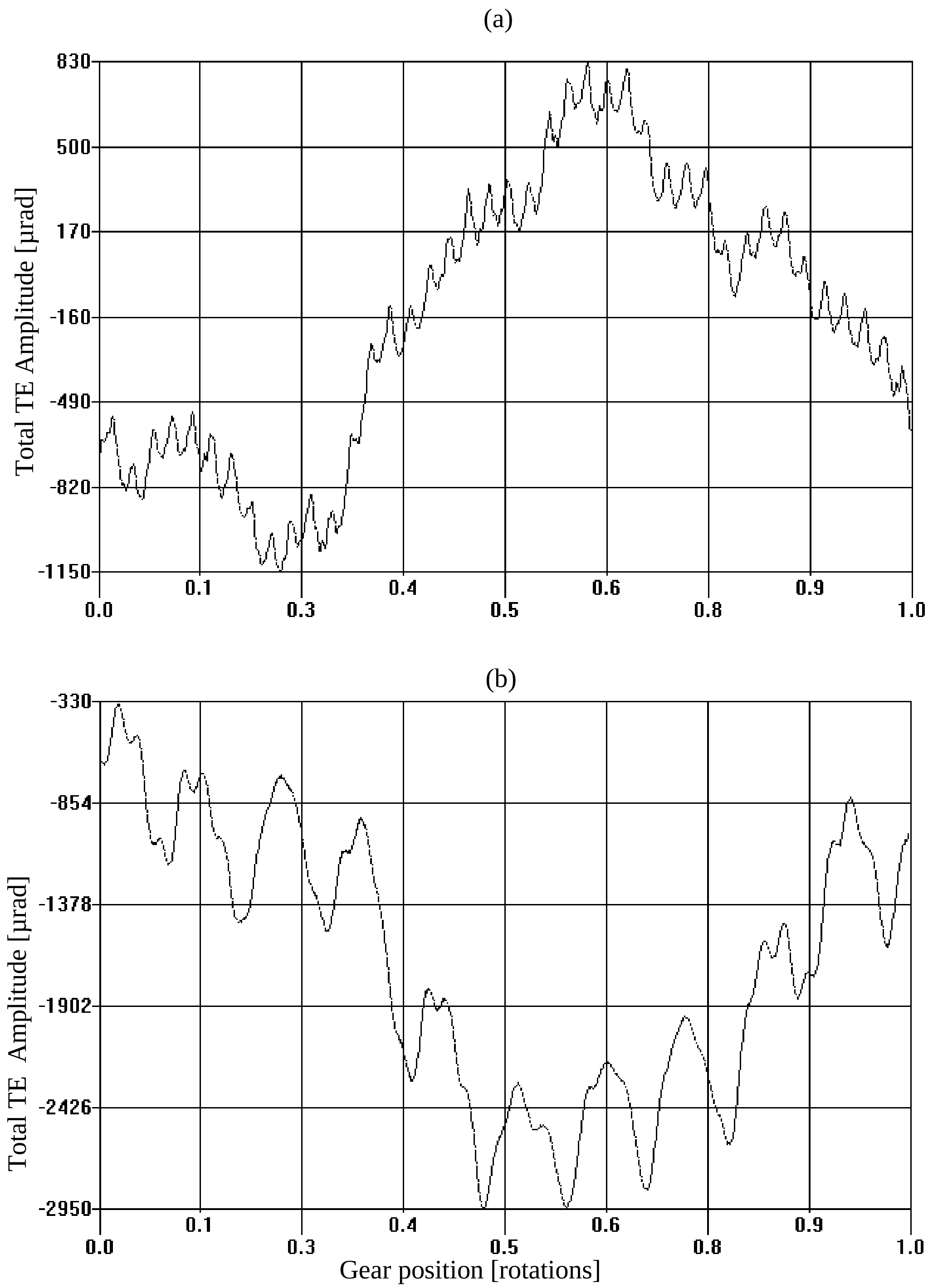

Figure 13: An example set of TE time histories relative to (a) output and (b) input for the hypoid gear set operated under drive conditions at an input torque of 300 Nm and nominal assembly position.

defined by Eq. (1) show very similar shapes, with the amplitudes are such that $TE_{in}(t) \approx \frac{N_g}{N_p} TE_{out}(t)$, as described in Chapter 2.

The data analysis software provides a low-pass filtered version of the TE data to show the impact of once-per-revolution type gear effects such as roundness and run-out errors and spacing and indexing errors. The cut-off frequency is below the gear mesh frequency ($f_{mesh} = \frac{1}{2\pi} N_p \omega_p = \frac{1}{2\pi} N_g \omega_g$ in Hz where ω_p and ω_g are the rotational speeds of the pinion (input) and the gear (output), both in rad/s) in this case such that gear mesh related fluctuations are filtered out. At the input speed value of 15 rpm used in the experiments, the cut-off frequency for the low-pass filter was set to a value less than $f_{mesh} = 2.5$ Hz. Figure 14(a) shows a low-pass filtered $TE_{out}(t)$ signal corresponding to total TE signal of Figure 13(a). Likewise, a high-pass filter was also applied to the same signal at the same cut-off frequency to retain the mesh frequency components while filtering out all once-per-revolution effects. The high-pass filtered version of the same data is shown in Figure 14(b). It is noted from Fig 15(a) that the low-pass filtered TE does not repeat itself for every output rotation. This is expected since the gear ratio is 4.1:1 (i.e. 4.1 pinion rotations take place for each gear rotation). As low frequency TE components are attributable to both pinion and gear errors, one would expect the low-pass filtered TE to repeat itself for every 10 output rotations, which represents a complete

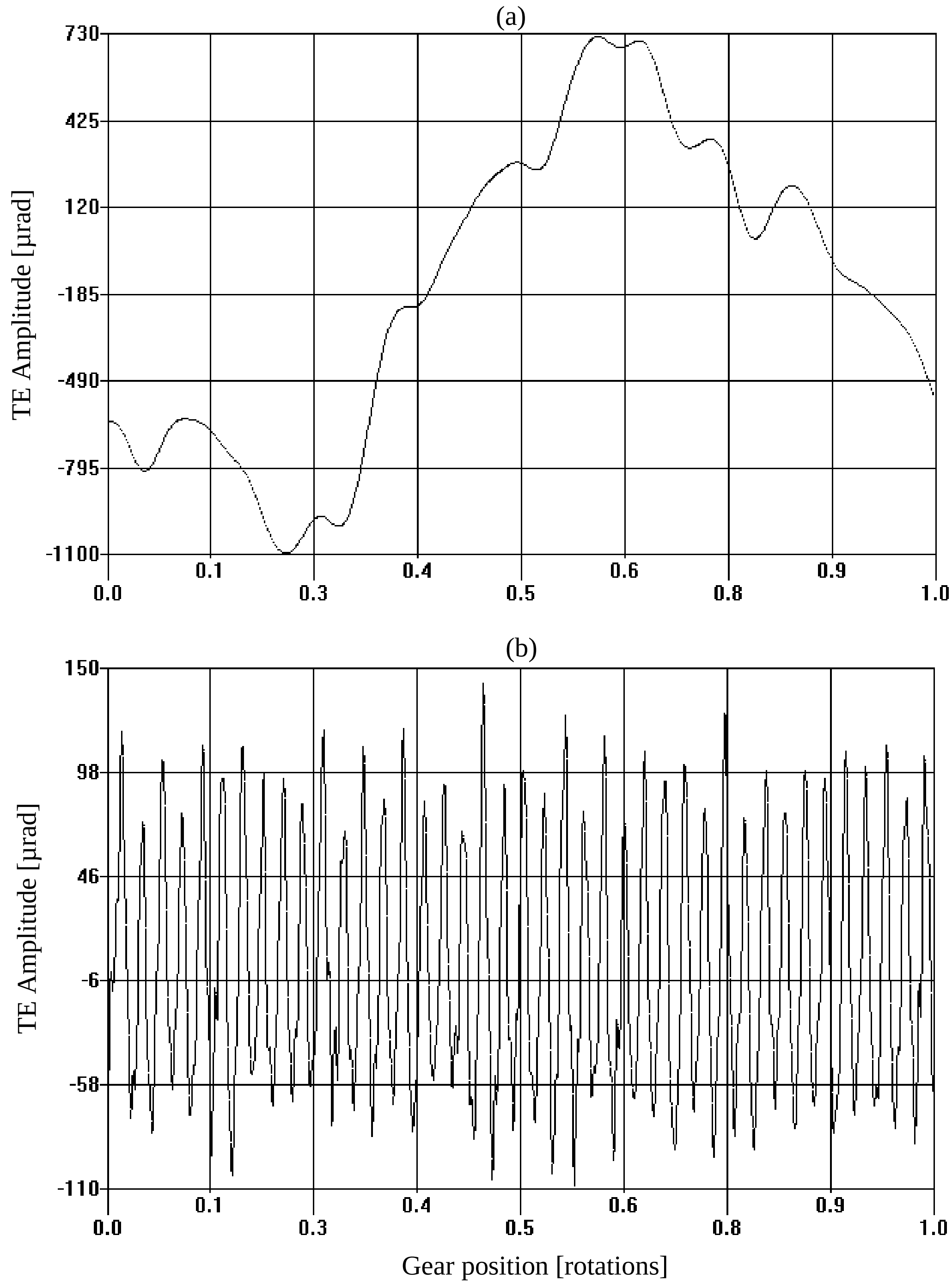

Figure 14: (a) Low-pass and (b) high-pass filtered signals obtained from the output TE of Figure 13(a)

period of the gear set. Also noted in Figure 14(b) is 41 fluctuations per output rotation each representing one mesh cycle.

The FFT spectra corresponding to the output and input TE time histories of Figure 13(a) and (b) are shown in Figure 15(a) and (b), respectively. In these spectra, the frequency axes were normalized with respect to the rotational frequencies of the output and the input ($f_{out} = \omega_g / 2\pi$ and $f_{in} = \omega_p / 2\pi$), respectively. In the case of the output TE spectrum of Figure 15(a), $H_m = f_{mesh} / f_{out} = N_g = 41$ is the first gear mesh order while $H_{2m} = 2H_m = 82$ and $H_{3m} = 3H_m = 123$ represent the second and third gear mesh harmonic amplitudes of the TE signal, respectively. Likewise, the input TE spectrum of Figure 15(b) has its frequency axis normalized by f_{in} such that $H_m = f_{mesh} / f_{in} = N_p = 10$, $H_{2m} = 2H_m = 20$ and $H_{3m} = 3H_m = 30$. It is noted, for instance, H_{1m} values relative to output and input are about 319.5 and 75.8 μrad, representing a ratio very close to the speed ratio of 4.1.

Meanwhile, shaft orders on the output spectrum are $H_{sp} = 4.1$ and $H_{sg} = 1$ in Figure 15(a) while they are $H_{sp} = 1$ and $H_{sg} = 1/4.1 = 0.2439$ in Figure 15(b) for input orders.

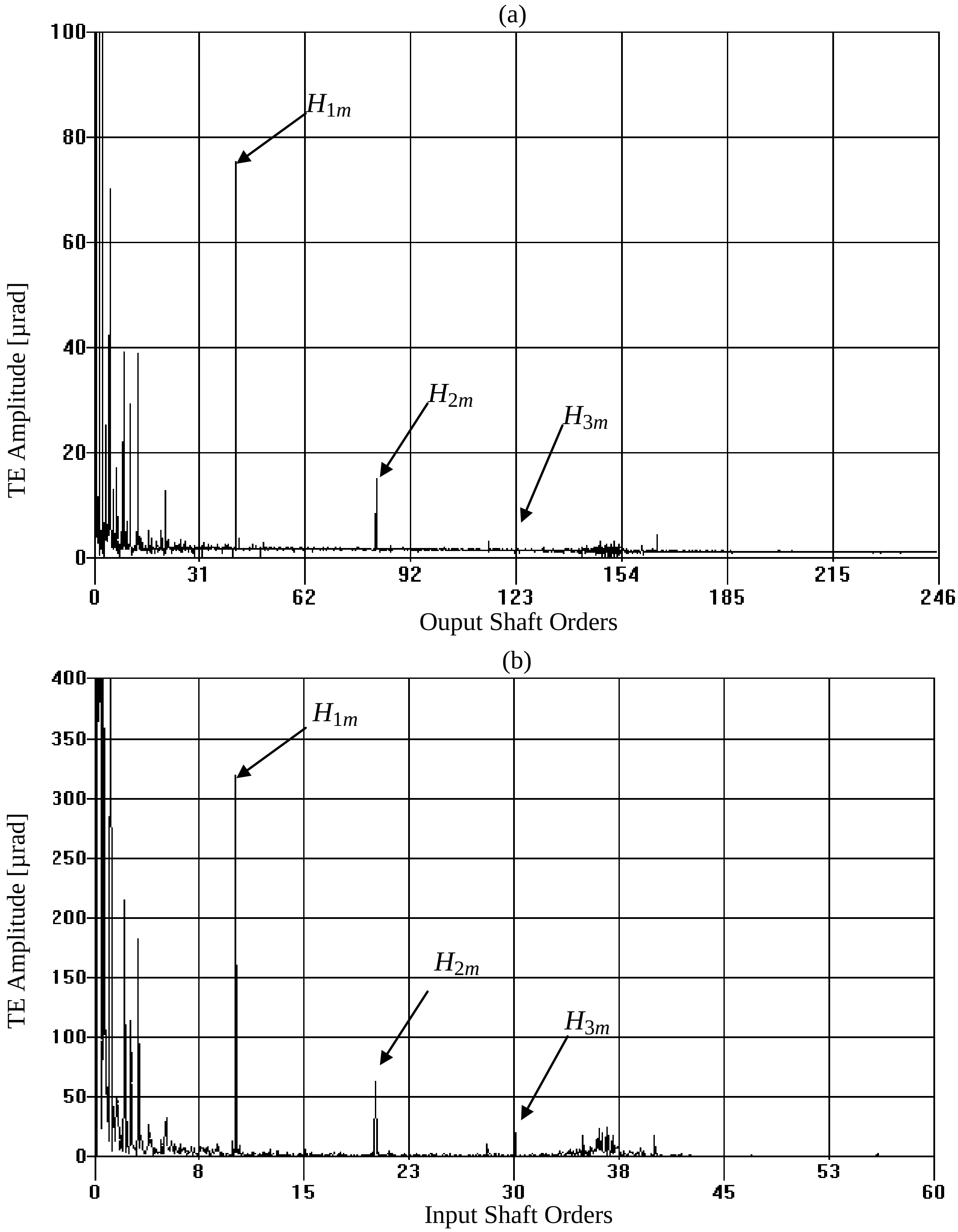

Figure 15: (a) Output order and (b) input order TE spectra corresponding to the TE time histories of Figures 16(a) and (b), respectively.

3.3 Repeatability of the Experiments

In order to be able to associate the measured changes in loaded transmission error values to certain position errors, which is the major goal of this study, repeatability of the system (including the test machine with its fixtures and assembly variations, encoder-based measurement system and the data analysis method) must be demonstrated first.

For checking for the repeatability of the system, the same test was repeated at different load levels (100, 200, 300, 400 and 450 Nm) using a pair of hypoid gears having the same design as the example test gears. These tests were run on different days with tear-downs in between. Figure 16 compares the first gear mesh harmonic amplitude A_{1m} of the transmission error at order H_{1m} from two such tests. It is seen that the maximum variability of about 5% is observed at the mid-range loads of 300 and 400 Nm. All of the A_{1m} values of the second test are within about 3 μrad of the first test, indicating that the repeatability of the test set-up is indeed satisfactory.

3.4 Gear Pair Backlash Measurements

As detailed in Chapter 2, backlash measurements were done for each position error configuration. After setting the nominal backlash value of 0.1 mm for the no-error case, actual backlash values for tests with different error values were all measured and

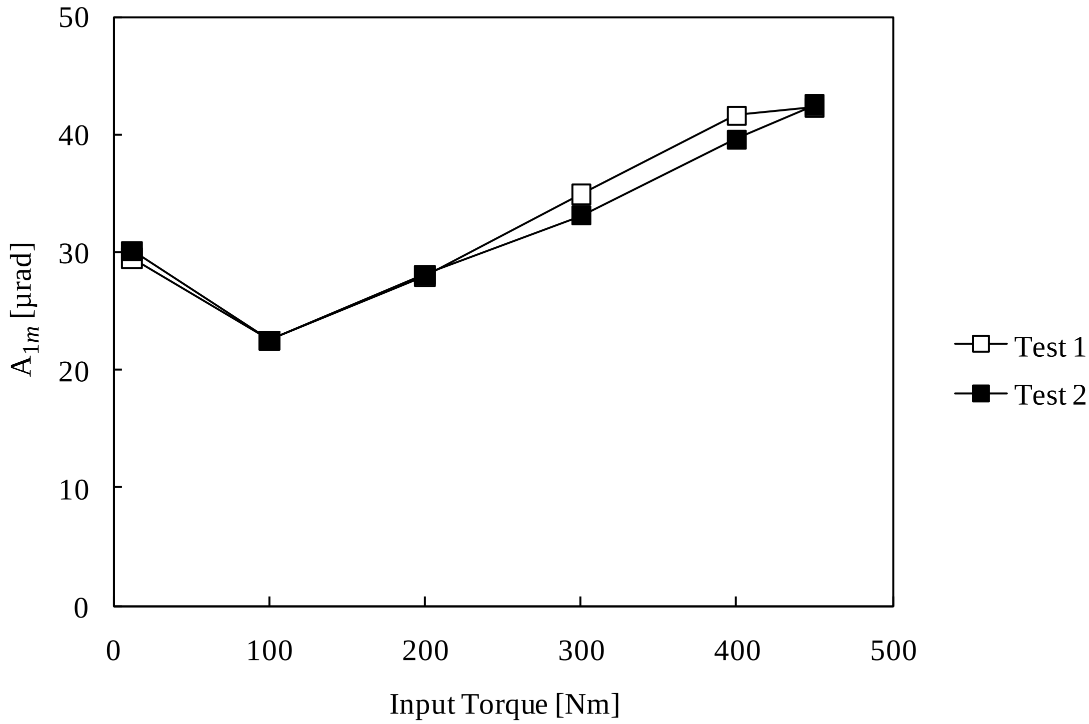

Figure 16: Comparison of the first harmonic amplitude A_{1m} of the transmission error from a pair of repeatability tests.

recorded using the procedure outlined in Chapter 2. Any cases that resulted in zero backlash value (tight-mesh conditions) were removed from the test matrix.

The backlash measurements are summarized in Figure 17 for the example test gear pair. Starting with the set value of 0.1 mm for the case when $H = V = G = 0$ mm and $\gamma = 0^\circ$, backlash values are observed to reduce with introduction of errors in negative direction (as defined in Figure 5). The shaft angle error value of $\gamma = -0.2^\circ$ result in zero backlash while $\gamma = 0.2^\circ$ result in 0.53 mm backlash. The impact of the G error on backlash is also seen to be very significant, as expected where a backlash range of 0.11 to 0.51 mm is obtained by varying the gear position error within the range $G = -0.05$ to 0.3 mm. On the other hand, the influence of the V error on backlash is the least significant as a backlash range of 0.11 to 0.24 mm is obtained for $V = -0.2$ to 0.2 mm.

Since it resulted in zero backlash value, error condition of $\gamma = -0.2^\circ$ (i.e. shaft angle of 89.8°) was excluded from the test matrix.

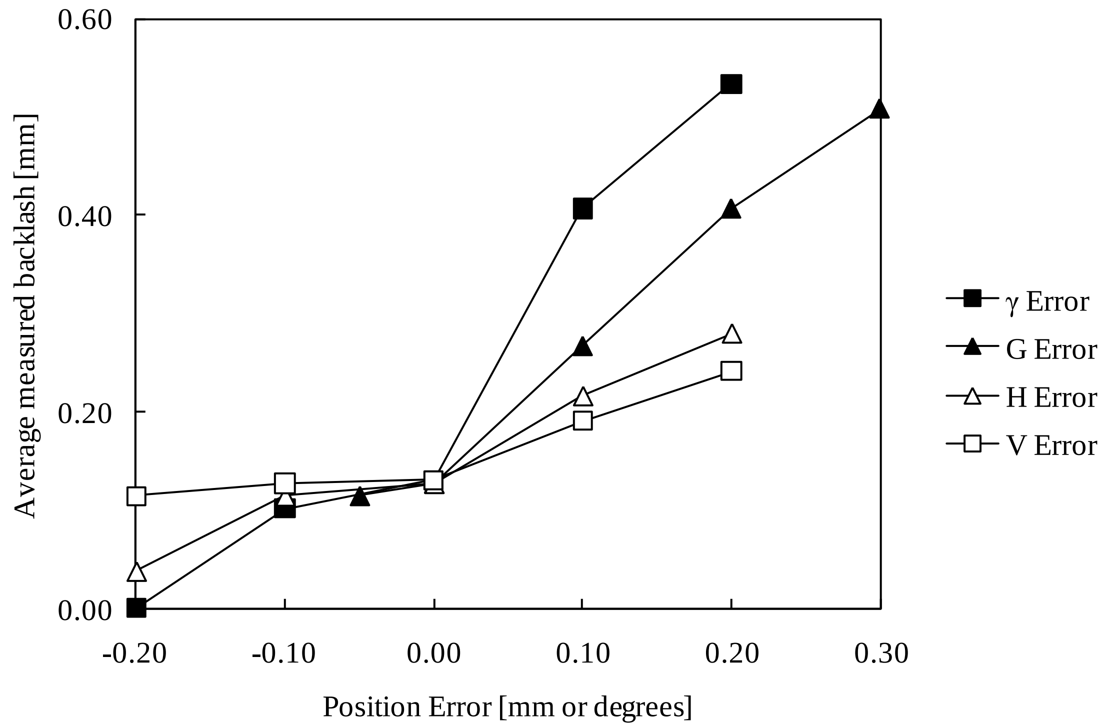

Figure 17: Measured backlash values versus the various position errors of the hypoid gear set.

3.5 Transmission Error Test Results

3.5.1 Influence of Torque on the Transmission Error

The loaded transmission error has two components. One component is geometry related, originating from the surface deviations. When the gears are rolled without any torque transmitted, this deviation component is the sole contributor to the transmission error. Such deviations are present in the test gears since they are face-hobbed and lapped. The second component is due to deflection of teeth, contacts and gear blanks under load. As in spur and helical gears, hypoid gear surface deviations induced by lapping can be off-set at a certain "design" torque to minimize transmission error.

In order to quantify such torque effects, the gear pair was tested under no position error condition at various torque values ranging from 0 and to 500 Nm. Figure 18 shows the measured variation of the first three gear mesh harmonics (A_{1m}, A_{2m} and A_{3m}) of the transmission error with input torque when the gear pair is operated under drive conditions. In Figure 18(a), the curves are plotted within the entire torque range while Figure 18(b) zooms in A_{1m} within the range up to 100 Nm. A V-shaped behavior is evident here where the transmission error harmonics (especially A_{1m}) first reduce and then increase in an almost linear manner with input torque. Here $A_{1m} = 33$ μrad at the lowest torque value of 6 Nm (minimum amount of torque achievable when the output

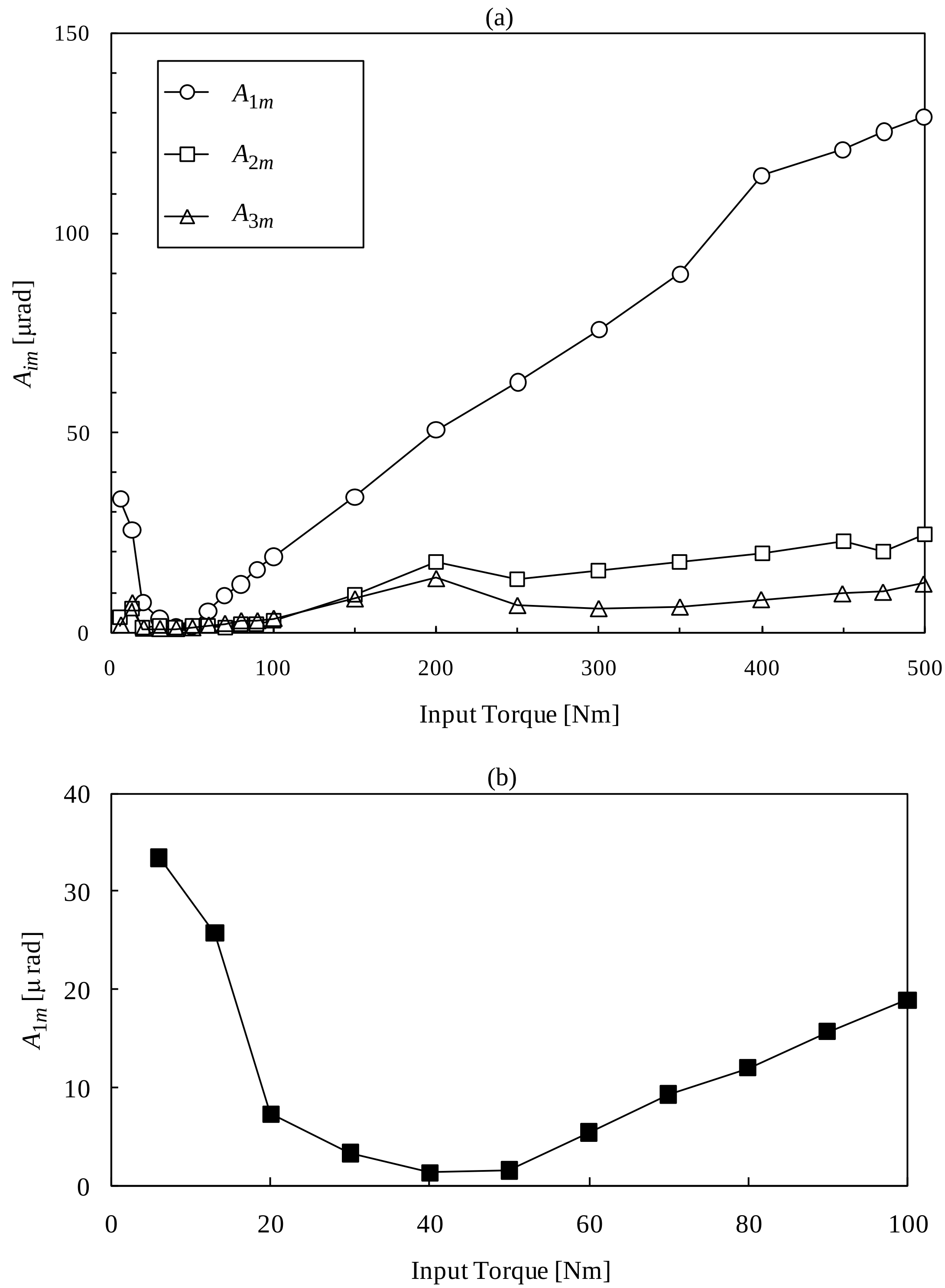

Figure 18: (a) Measured variation of A_{im} ($i = 1-3$) with input torque, and (b) a close up view of the A_{1m} curve in the low load range. The gear set is operated under drive conditions.

side is totally disengaged). It goes down to its minimum of 1.3 μrad at 40 Nm, beyond which it increases in an almost linear manner. At 500 Nm, A_{1m} is nearly 130 μrad. The higher harmonics, while following the same trend as the first harmonics, have significantly lower values. For instance, at 500 Nm, $A_{2m} = 24.4$ μrad and $A_{3m} = 12.2$ μrad, that are both significantly less than A_{1m}.

Figure 19 shows the corresponding results for the coast side using the same format as Figure 18. While the unloaded transmission error value of $A_{1m} = 32$ μrad is almost the same as that of the drive conditions, two local mimima are evident in Figure 19, one at 10 Nm and one at 60 Nm. Since the coast side surfaces of the hypoid gear pair are not lapped (as hobbed only), such qualitative differences can be expected. If the first dip in the A_{1m} curve is overlooked, the rest of the curve (from 30 Nm on) has the same qualitative V-shape as the drive side curves. All three harmonics of the transmission error under the coast conditions are higher than those under the drive conditions. For instance, at 500 Nm, $A_{1m} = 177.9$ μrad under the coast conditions, a nearly 40% increase compared to the drive side value.

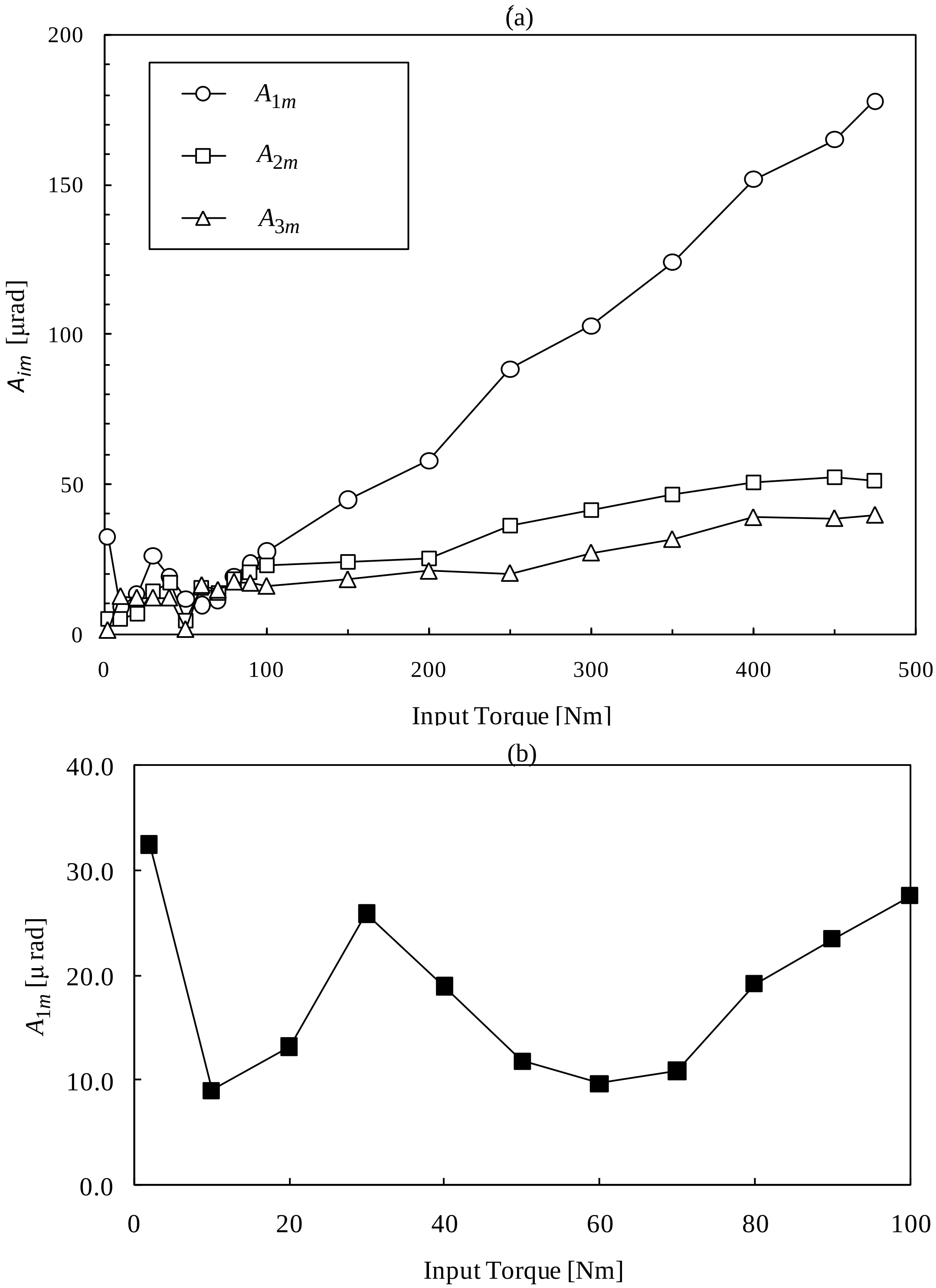

Figure 19:(a) Measured variation of A_{im} ($i = 1-3$) with input torque, and (b) a close up view of the A_{1m} curve in the low load range. The gear set is operated under coast conditions.

3.5.2 Influence of the *H* error on the Transmission Error

As listed in the test matrix of Table 2, sets of tests with horizontal pinion errors were performed under both drive and coast conditions. In these tests, error values of $H = -0.2, -0.1, 0, 0.1$ and 0.2 mm were used with all other $V = G = \gamma = 0$. Figure 20(a) shows the variation of the first harmonic amplitude of the transmission error (A_{1m}) with *H* under different values of input torque with drive side operation. It can be seen in this figure that A_{1m} overall shows slight upward trend as *H* is increased from -0.2 to 0.2 mm. A similar trend was observed in Figure 17 in terms of backlash value as well. The trend for the (almost) unloaded case is however opposite where A_{1m} reduces with increasing *H*. Overall, the observed variations of the transmission error with *H* are rather small.

In Figure 20(b), the same data as Figure 21(a) are presented as to show the variation of A_{1m} with torque at different values of *H*. The same V-shaped dependence on torque reported in the previous section for the case of zero position errors is evident here for the cases with H errors as well, except $H = 0.2$ mm when backlash is nearly 2.5 times its nominal value.

The coast side data corresponding to those presented in Figure 20 is given in Figure 21. In this figure, it is seen that that *H* value, within the range considered, has very little or no impact on A_{1m}. In Figure 21(a), A_{1m} versus *H* curves have almost zero

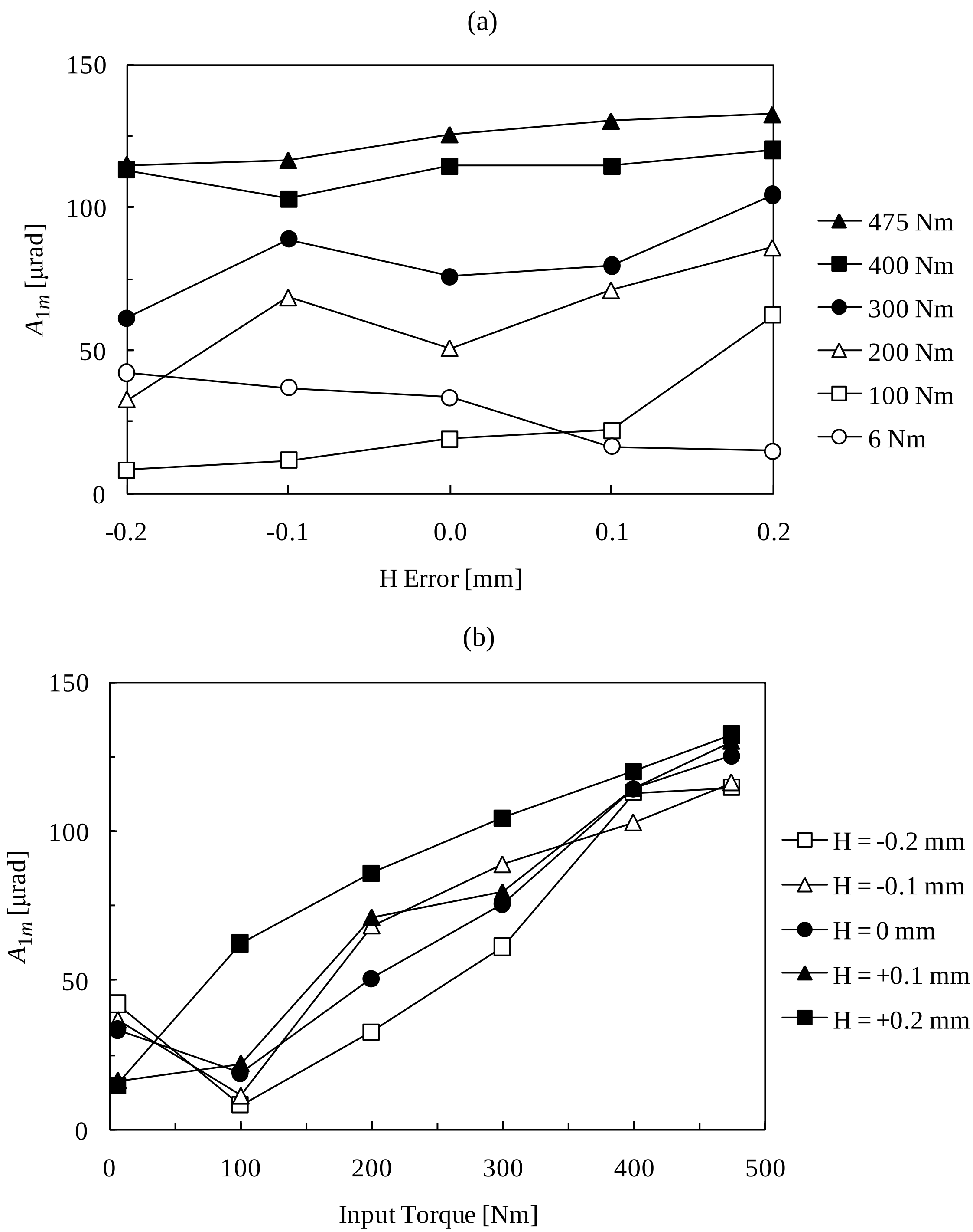

Figure 20: Variation of the first harmonic amplitude of TE (a) with the *H* error at various input torque values and (b) with input torque at various *H* values. The gear set is operated under drive conditions.

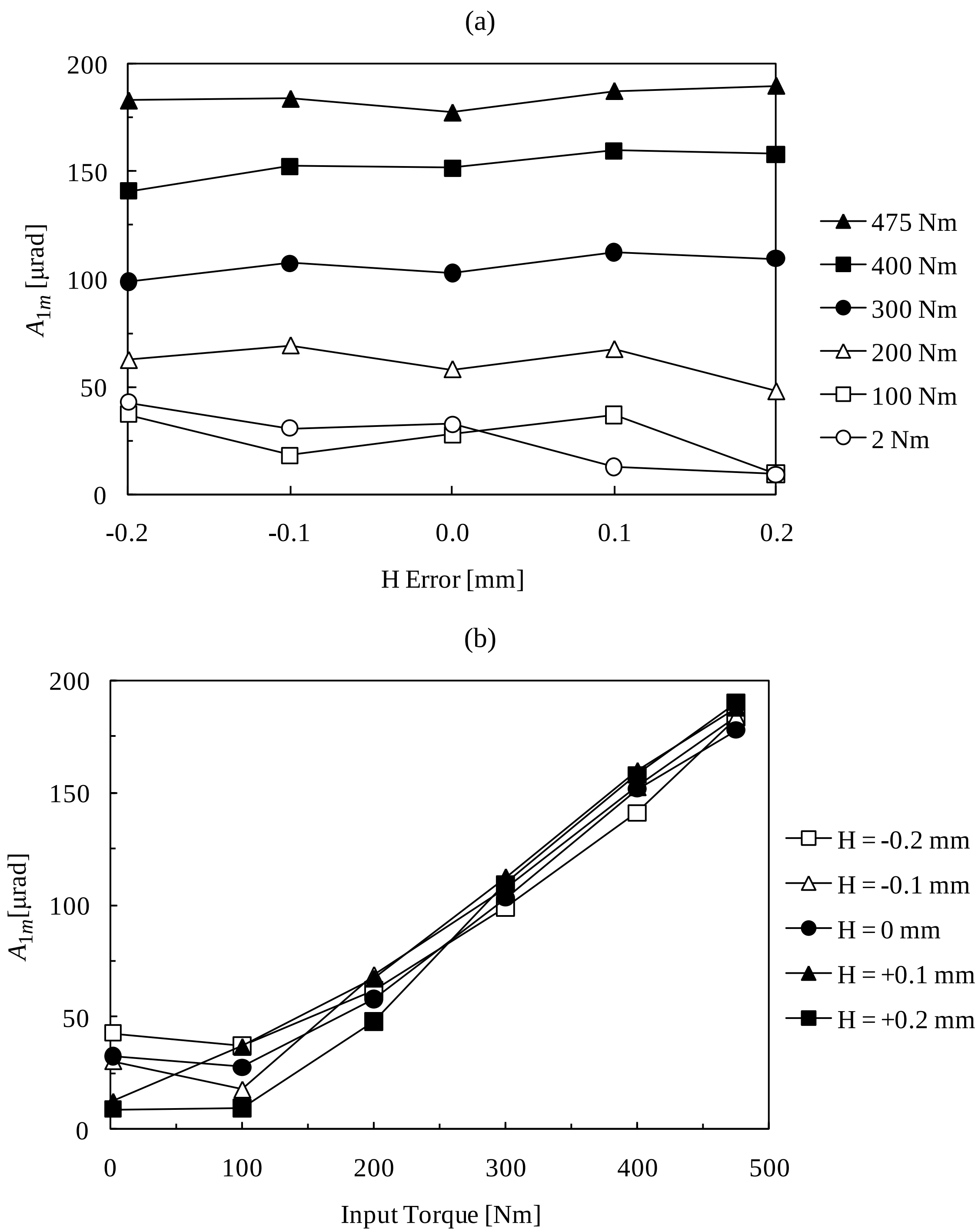

Figure 21: Variation of the first harmonic amplitude of TE (a) with the *H* error at various input torque values and (b) with input torque at various *H* values. The gear set is operated under coast conditions.

slope under loaded conditions while a slight reduction in unloaded A_{1m} values is evident with increasing *H*.

3.5.3 Influence of the *V* error on the Transmission Error

Next, the influence of the shaft off-set error *V* will be investigated using the same example gear pair through tests with error values of $V = -0.2, -0.1, 0, 0.1$ and 0.2 mm and $H = G = \gamma = 0$. These tests were performed under drive and coast conditions as well. Figure 22(a) documents the variation of A_{1m} with *V* under six different input torque values ranging from unloaded to 500 Nm during the drive side operation. It is observed that the value of A_{1m} changes in a slight manner with *V*. An increase of this error from -0.2 to 0.2 mm appears to increase A_{1m} slightly under highly loaded conditions (e.g. at 400 and 475 Nm) while a consistent trend is not observed at lower torque ranges. In Figure 22(b), the same data as Figure 22(a) is presented as to show the variation of A_{1m} with torque at different *V*. These V-shaped curves for different *V* values are rather close to each other pointing to the limited influence of applying *V* errors only.

Figure 23 shows the coast side data corresponding to those presented in Figure 22. Here, the influence of the value of the *V* error is more prominent. For all of the loaded cases, applying a negative *V* error consistently decreases A_{1m} while a positive *V* does the

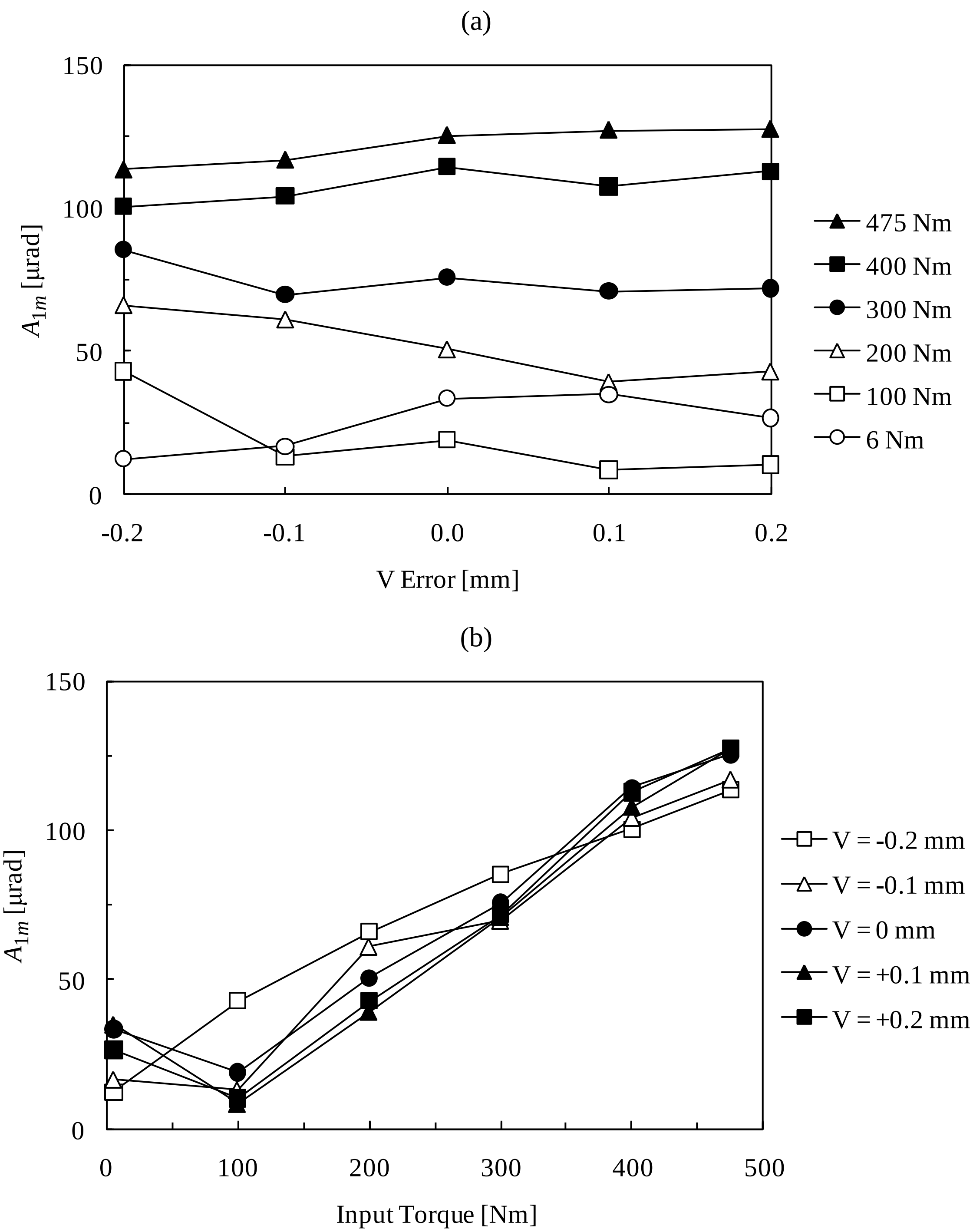

Figure 22: Variation of the first harmonic amplitude of TE (a) with the *V* error at various input torque values and (b) with input torque at various *V* values. The gear set is operated under drive conditions.

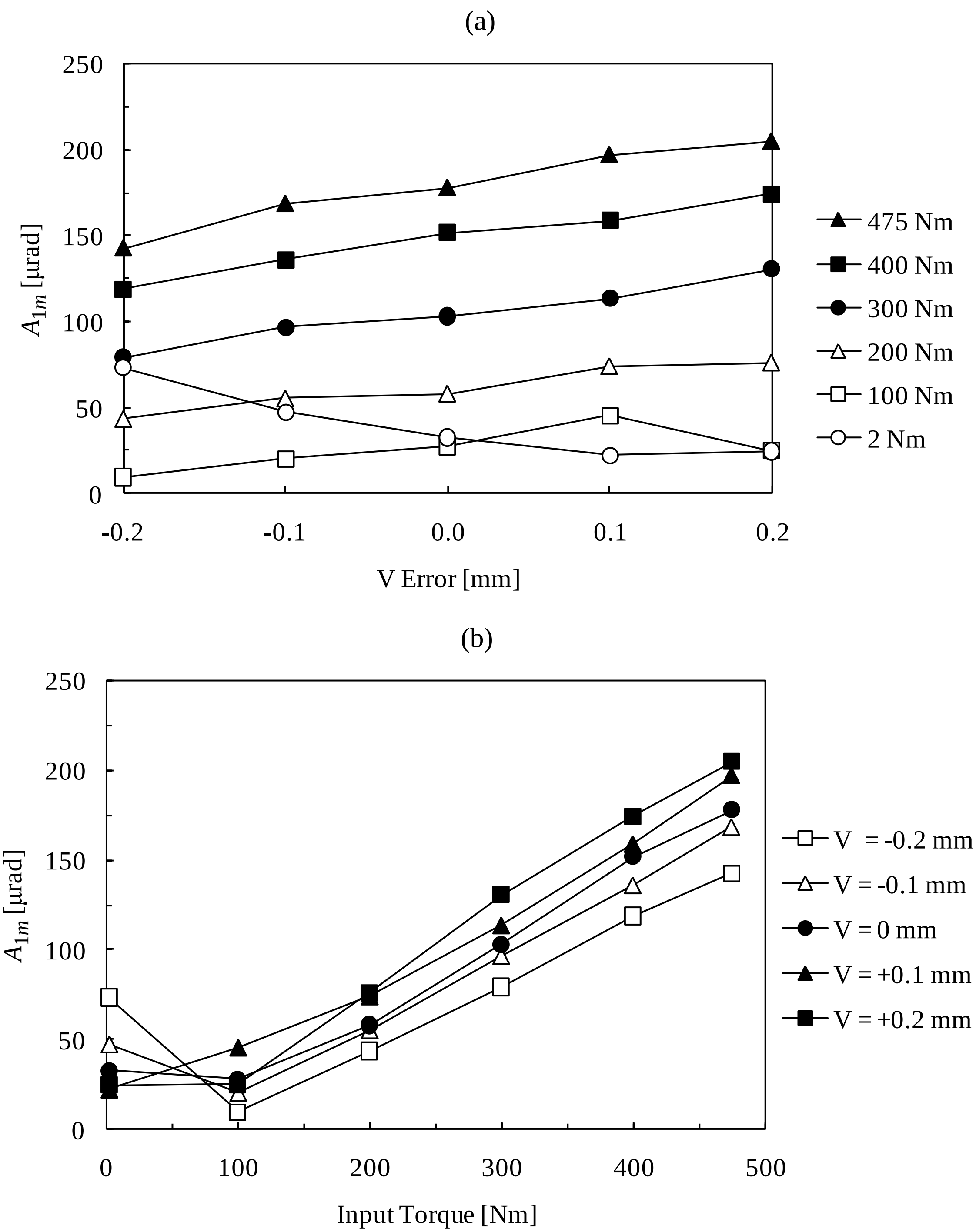

Figure 23: Variation of the first harmonic amplitude of TE (a) with the *V* error at various input torque values and (b) with input torque at various *V* values. The gear set is operated under coast conditions

.

opposite. For instance, at 475 Nm, $A_{1m} = 177.9$ μrad for $V = 0$ while $A_{1m} = 142.6$ and 205.1 μrad (20% lower and 15% higher) at $V = -0.2$ and 0.2 mm, respectively. It is also noted in the same figure that the trend for the almost unloaded case is the opposite of the one for the loaded cases.

3.5.4 Influence of the *G* error on the Transmission Error

Figure 24 shows the influence of *G* errors on transmission error during drive side operation of the gear set. Here, $G = -0.05, 0, 0.1$, 0.2 and 0.3 mm and $H = V = \gamma = 0$. It can be seen in Figure 24(a) that the *G* error has very little effect on A_{1m} at higher torque ranges, say at and above 400 Nm for this example gear set. At lower torque values, minimum transmission error amplitudes are obtained at $G = 0$, while increasing moving the gear in either direction away from the nominal zero position is seen to increase A_{1m} slightly. For instance, at 200 Nm, $A_{1m} = 50.6$ μrad for $G = 0$, compared to $A_{1m} = 70.2$ μrad (40% higher) for $G = -0.05$ mm and $A_{1m} = 73.8$ μrad (40% higher) for $G = 0.3$ mm. In Figure 24(b), the same data as Figure 24(a) is presented as to show the variation of A_{1m} with torque at different *G* values. Again, most of the *G* values considered with the exception of $G = -0.05$ mm reveal V-shaped curves with a minimum A_{1m} at 100 Nm.

(a)

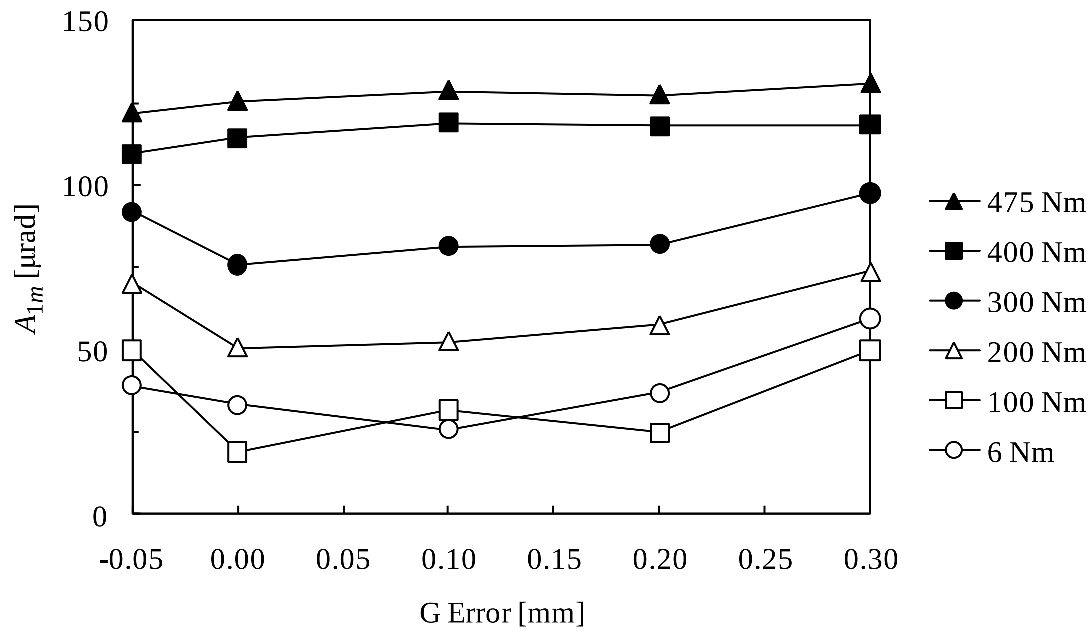

(b)

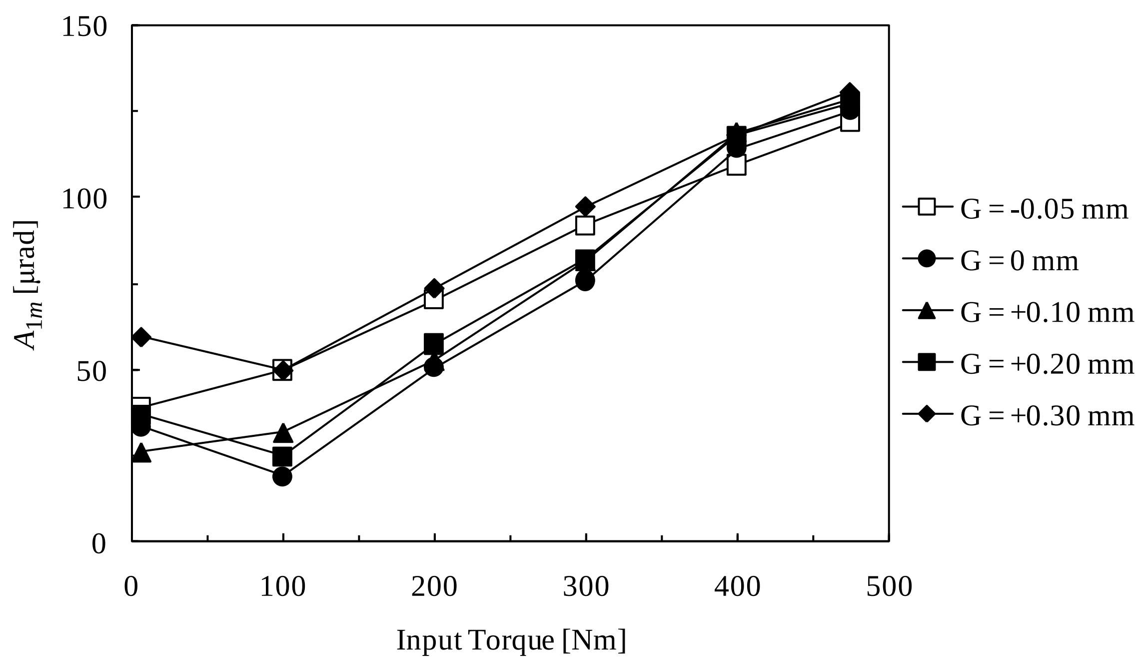

Figure 24: Variation of the first harmonic amplitude of TE (a) with the *G* error at various input torque values and (b) with input torque at various *G* values. The gear set is operated under drive conditions.

Also noted in this figure, that the curves for different *G* values are more separated at lower *G* values while they merge as *G* is increased.

Figure 25 shows the coast side data corresponding to those presented in Figure 24. Here, the influence of the value of the *G* error still appears to be secondary. Figure 25(a) does not reveal any obvious trends in regards to the influence of the *G* error.

3.5.5 Influence of the γ error on the Transmission Error

Finally, measurement results on the influence of the shaft error are presented in this section. While the test matrix of Table 2 called for five values of the shaft angle error, $\gamma = -0.2, -0.1, 0, 0.1$ and 0.2 degrees, tests were not performed at $\gamma = -0.2$ since the backlash value was zero according to Figure 17. For the remaining four γ values, Figure 26 shows the combined influence of input torque and the γ error on the first harmonic of the transmission error A_{1m} during drive side operation of the example gear set. It can be clearly seen in Figure 26(a) that as the γ error increased from -0.1° to 0.2° that the loaded transmission error increases significantly with the exception of the unloaded case (6 Nm) where an opposite trend is evident. For instance, at 475 Nm, $A_{1m} = 114.6$ μrad at $\gamma = -0.1^{\circ}$ while it is 145.8 μrad at $\gamma = 0.2^{\circ}$ showing a 27% increase. It must also be recalled that the γ error had the greatest influence on the measured

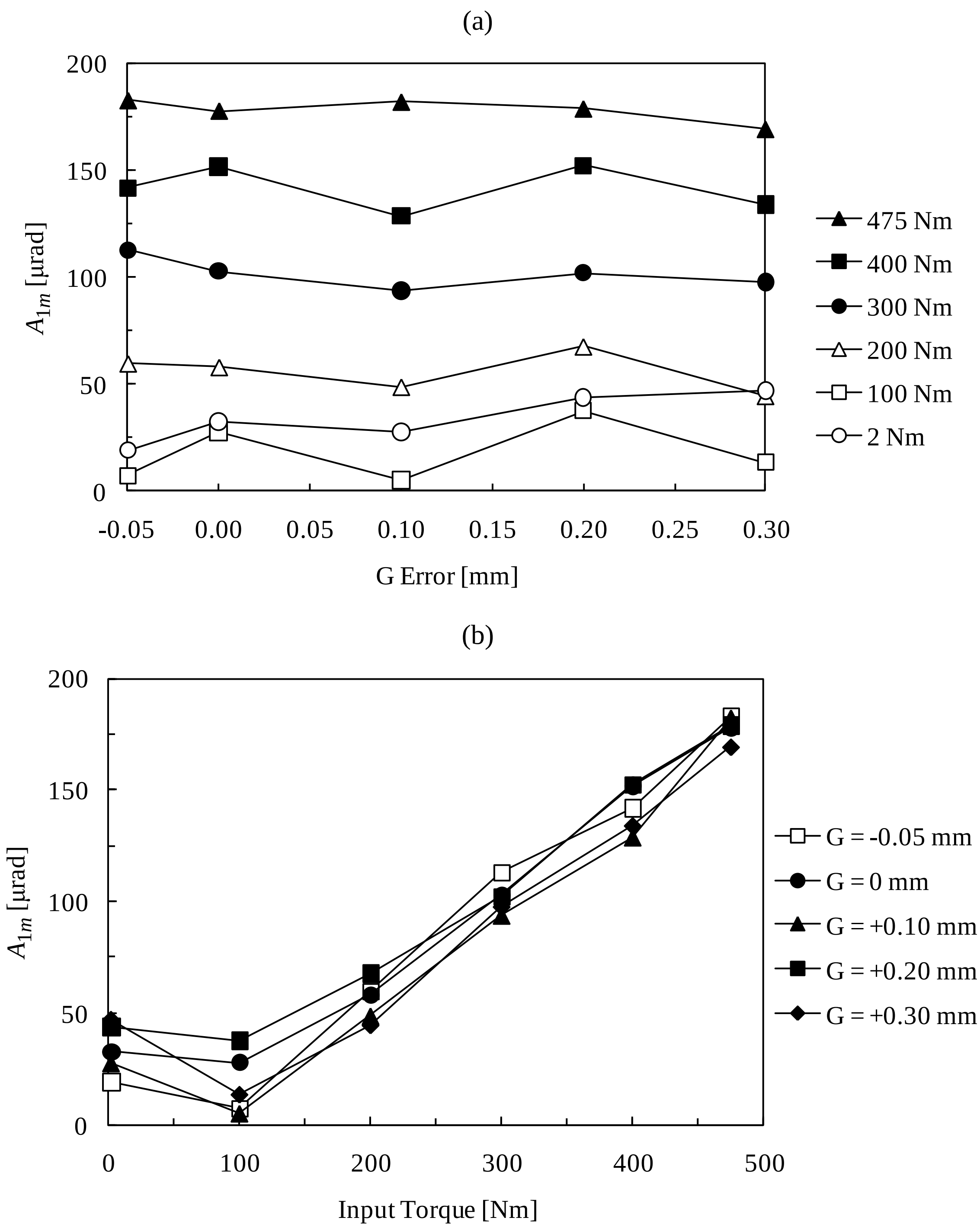

Figure 25: Variation of the first harmonic amplitude of TE (a) with the *G* error at various input torque values and (b) with input torque at various *G* values. The gear set is operated under coast conditions.

(a)

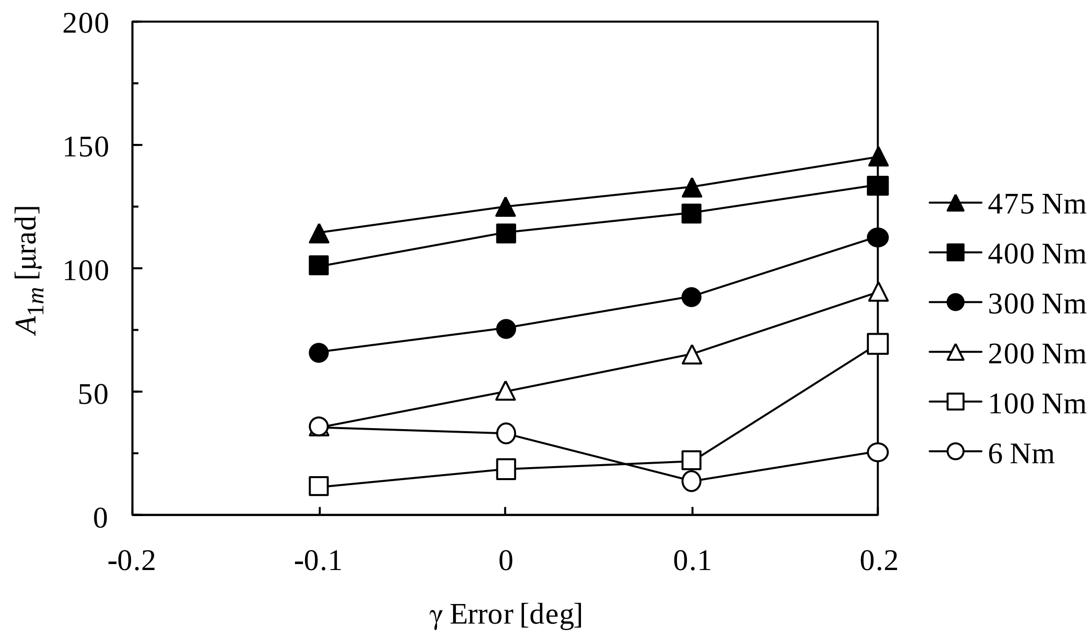

(b)

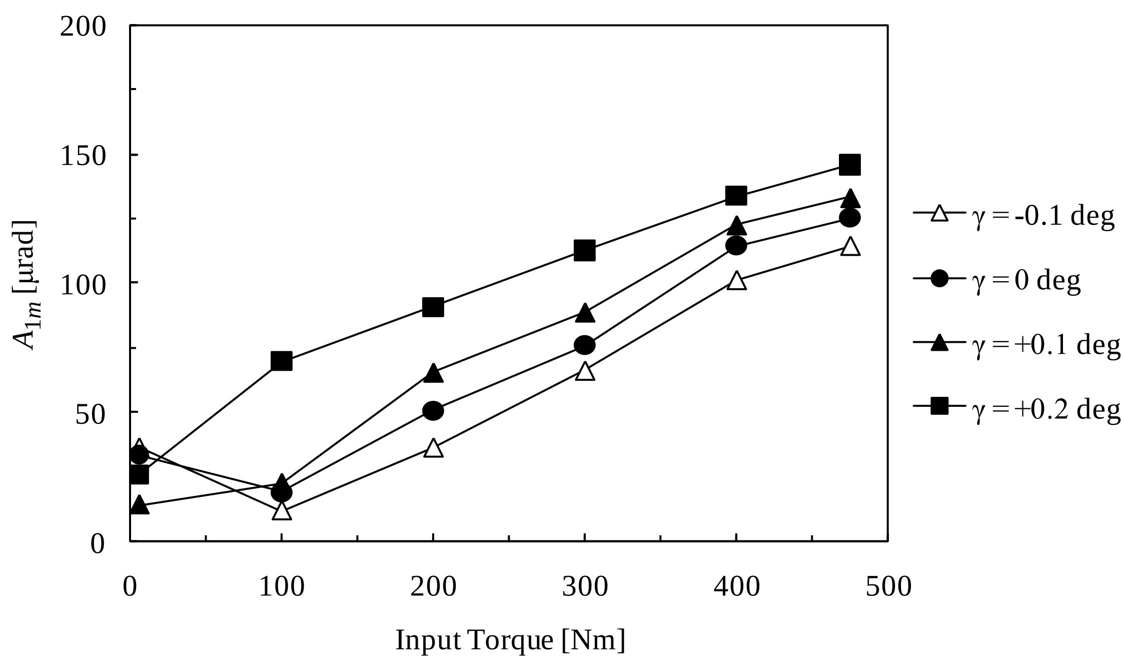

Figure 26: Variation of the first harmonic amplitude of TE (a) with the γ error at various input torque values and (b) with input torque at various γ values. The gear set is operated under drive conditions.

backlash as well. In Figure 26(b), the transmission error is plotted against the input torque for various γ errors. These curves generally reflect the same behavior as seen in Figure 18 for the no error position. They show a dip at a load of 100 Nm, and beyond that, they continuously increase. An exception to this behavior is seen for $\gamma = +0.2°$, where there is no dip at a load of 100 Nm, possibly due to very high backlash value. It is also seen in Figure 26(b) that curves for each γ value are well separated within the entire torque range, further iterating the sensitivity of the motion transmission error of a hypoid gear pair to shaft angle errors.

The same level of influence of γ was observed during the coast side operation of the same gear pair as well as shown in Figure 27. The major difference between the drive side (Figure 26(a)) coast side (Figure 27(a)) results is that the A_{1m} amplitudes decrease in coast as γ error increased from -0.1° to 0.2°. For a load of 475 Nm, A_{1m} was 185 to 146 μrad for these two limiting γ values representing a 20% spread.

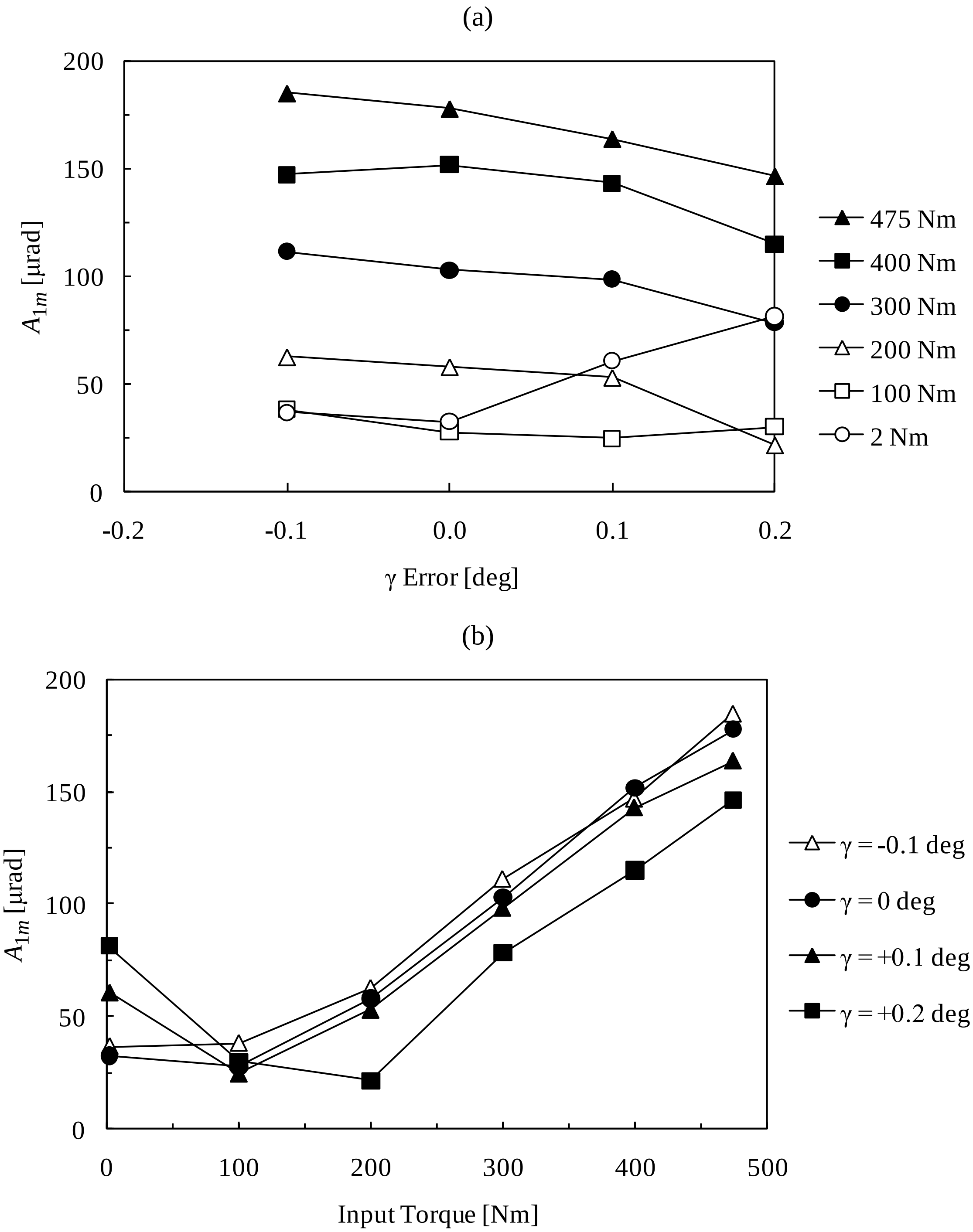

Figure 27: Variation of the first harmonic amplitude of TE (a) with the γ error at various input torque values and (b) with input torque at various γ values. The gear set is operated under coast conditions.

CHAPTER 4

SUMMARY AND CONCLUSIONS

4.1 Summary

In this thesis, an experimental investigation was performed to quantify the loaded static transmission error of a hypoid gear pair in the presence of various gear position errors. A test machine was developed to allow operation of a hypoid gear pair under a given constant torque and a very low rotational speed. The test set-up was incorporated with several adjustment mechanisms to induce any type of misalignment at any user defined magnitude. These mechanisms allowed application of pinion (H), gear (G), shaft off-set (V) and shaft angle (γ) errors independent of each other in a tightly controlled manner.

An encoder-based transmission error measurement system was designed and incorporated with the test machine. It employed two high-precision angular optical encoders, one connected to the input spindle and one to the output spindle, whose signals were processed in a special-purpose analyzer to obtain the transmission error in both time and frequency domains.

A detailed test matrix that included various types and magnitudes of misalignments, drive and coast side conditions as well as a wide range of input torque was defined and executed by using an example rear axle hypoid gear pair. Additional tests were conducted to demonstrate the repeatability and accuracy of the test rig, measurement system and the test processes devised. The test results were presented in the form of variation of the first three harmonic amplitudes of the transmission error as a function of torque and error amplitudes. It was shown the each misalignment impacts the transmission error in different levels. The drive and coast side transmission error measurements were shown to differ as well. A nearly “V-shaped” dependence of the first harmonic amplitude of the transmission error to the torque transmitted was also documented regardless of the error types and values applied to the gear pair.

4.2 Conclusions

Based on the repeatability and performance of the test set-up and instrumentation developed in this study, it can be concluded that the experimental methodology proposed is indeed effective and accurate in measuring the transmission error of a hypoid gear pair under loaded and quasi-static conditions. The repeatability of the data in the presence of various types and magnitudes of error also indicates that the novel idea implemented here to apply position errors is also very effective. For these reasons, the test set-up and the measurement system developed in this study can be considered as one of the main contributions of this study to the state-of-art from the measurement and testing point of view.

In terms of the overall behavior of the measured transmission error data, following main conclusion can be made:

- The dependence of the transmission error harmonic amplitudes to the torque transmitted is quite well-defined. The transmission error amplitudes measured under no load decrease significantly with an increase in load, reaching their minimum values at a torque value (design load) less than 100 Nm beyond which the transmission error amplitudes increase almost linearly. Such a "v-shaped" dependence was demonstrated for modified parallel-axis gears as well [18]. While this behavior remained the same for every error configuration, the value of the design load was shown to be influenced by the error type and magnitude. As the example hypoid gear pair was a lapped face-hobbed gear pair, such dependence to torque is expected.

- With an increase in *H* position error as the pinion is moved away from the gear along its axis of rotation, the transmission error increased slowly for both drive and coast side operations reflecting the behavior of the backlash as well.

- An increase in the *V* error representing an increase in shaft off-set was shown to increase the transmission error amplitudes slightly for both drive and coast side operations in a manner very similar to that of the *H* error.

- An increase in backlash of the gear pair by increasing the *G* error (i.e. by moving the gear away from the pinion along its rotational axis) was shown to result in slight increases of transmission error in drive side operation while a slight reduction was observed with the coast side operation.

- The transmission error amplitudes were shown to be influenced by the shaft error (γ) rather significantly. Increasing the γ error caused the transmission error amplitudes to increase significantly for the drive side operation. The opposite was observed during the coast side operation where an increase in γ resulted in significant reductions in the transmission error amplitudes.

- The coast side transmission error amplitudes were up to 40% higher than those for the drive side operation regardless of the error type and magnitude.

4.3 Recommendations for Future Work

This study on the measurement of loaded static transmission error can be further expanded to meet additional objectives to advance our understanding of hypoid gears. The following are some recommendations for future work:

- *Expand test matrix to include combined position errors*: In this study, only one type of error was considered in a given test. Two or more position errors can be applied in combination to investigate their composite effect.

- *Tests for Hypoid gears with other applications*: As the test machine is applicable to gears of different sizes and ratios, additional tests can be performed with hypoid gear pairs to investigate the generality of the trends observed.

- *Tests under dynamic conditions*: In practice, the hypoid gears run at much higher speeds under the potential influence of dynamic effects. In this study, only the quasi-static behavior was investigated. As a natural extension of this work, a methodology can be developed to investigate the dynamic effects of hypoid gears.

- *Model correlation studies*: As stated in Chapter 1, there are several models that can predict the behavior measured in this study. Simulation of these tests using those models [2, 12] would provide much needed validation for building further confidence on them.

REFERENCES

[1] Stadtfelt, H.J., 1993. *Handbook of Bevel and Hypoid Gears*, Rochester Institute of Technology.

[2] Kolivand, M., 2009. "Development of Tooth Contact and Mechanical Efficiency Models for Face-Milled and Face-Hobbed Hypoid and Spiral Bevel Gears", Ph.D. Thesis, The Ohio State University, Columbus, Ohio.

[3] Kolivand, M. and Kahraman, A., 2009. "A Load Distribution Model for Hypoid Gears Using Ease-off Topography and Shell Theory", *Mechanisms and Machine Theory*, **44**, 1848-1865.

[4] Kolivand, M. and Kahraman, A., 2010. "An Ease-off Based Method for Loaded Tooth Contact Analysis of Hypoid Gears Having Global and Local Deviations", *Journal of Mechanical Design*, **132**, 071004 to 071004-8.

[5] Hotait, M., 2011. "A theoretical and Experimental Investigation of Root Stresses of Hypoid Gears with Misalignments", Ph.D. Thesis (in progress), The Ohio State University, Columbus, Ohio.

[6] Houser, D.R., and Blankenship, G.W., 1989. "Methods for Measuring Gear Transmission Error Under Load and at Operating Speeds", *SAE Technical Paper Series*, **98**, 1367-1374, Paper number 891869.

[7] Smith, J.D., 1983. *Gears and their Vibration*, The Macmillan Press Ltd., New York.

[8] Houser, D.R., 1992. "Gear Noise", Chapter 16 in Dudley's Gear Noise Handbook, D. Townsend, Editor, McGraw Hill.

[9] Houser, D.R., Oswald, F.B., Valco, M.J., Drago, R.J., and Lenski, J.W., 1994. "Comparison of Transmission Error Predictions with Noise Measurements for Several Spur and Helical Gears", *30th AIAA/ASME/SAE/ASEE Joint Propulsion Conference*, Indianapolis, IN, USA, June 27-29.

[10] Glover, R.C., and Rauen, D.G., 2003. "Gear Transmission Error Metric for Use with Gear Inspection Machine", SAE Paper 2003-01-1663.

[11] Artoni, A., Kolivand, M., and Kahraman, A., 2010. "An Ease-off Design Methodology for Optimization of the Loaded Transmission Error of Hypoid Gears", *Journal of Mechanical Design*, **132**, 011010-1 to 011010-9.

[12] *HypoidFaceHobbed* and *HypoidFaceMilled* Software Packages, Advanced Numerical Solutions Inc., Hilliard, OH, 2009.

[13] Gosselin, C., Cloutier, L., and Sankar, S., 1989. "Effects of the Machine Settings on the Transmission Error of Spiral Bevel Gears Cut by the Gleason Method", *Proc. 1989 Int. Power Transmission and Gearing Conference*, 705-712.

[14] Park, D., 2009. "Development of Surface Wear and lapping Simulation Models for Hypoid Gears", Ph.D. Thesis, The Ohio State University, Columbus, Ohio.

[15] Blankenship, G.W., Houser, D.R., and Carriere D.L., 1988. "The Development of a Variable Center Distance Gear Noise Test Facility", *AGMA Paper 88 FTM 13*.

[16] Tamminnana, V. K, Kahraman A. and Vijayakar, S., 2007. "On the Relationship between the Dynamic Factors and Dynamic Transmission Error of Spur Gear Pairs", *ASME Journal of Mechanical Design*, **129**, 75-84.

[17] Kahraman, A. and Blankenship, G. W., 1999. "Effect of Involute Contact Ratio on Spur Gear Dynamics", *ASME Journal of Mechanical Design*, **121**, 112-118.

[18] Kahraman, A. and Blankenship, G. W., 1999. "Effect of Involute Tip Relief on Dynamic Response of Spur Gear Pairs", *ASME Journal of Mechanical Design*, **121**, 313-315.

[19] Kahraman, A. and Blankenship, G. W., 1997. "Experiments on Nonlinear Dynamic Behavior of an Oscillator with Clearance and Time-varying Parameters", *ASME Journal of Applied Mechanics*, **64**, 217-226.

[20] Blankenship, G. W. and Kahraman, A., 1995. "Steady State Forced Response of a Mechanical Oscillator with Combined Parametric Excitation and Clearance Type Nonlinearity," *Journal of Sound and Vibration*, **185**, 743-765.

[21] Smith, J.D., 1987. "Gear Transmission Error Accuracy with Small Rotary Encoders", *Proceedings of the Institution of Mechanical Engineers*, **201** (C2), 134-135.

[22] Remond, D., and Play D., 1999. "Advantages and Perspectives of Gear Transmission Error Measurement with Optical Encoders", *4th World Congress on Gearing and Power Transmission*, Paris, France, March 16-18.

[23] Dziech, A.M., 1996. "Design of a Loaded Static Transmission Error Tester for Non-Parallel Axis Gearing", M. S. Thesis, The Ohio State University, Columbus, OH.

[24] Poling, G.R., 1999. "Hypoid Gear Test Rig Transmission Error Measurement Enhancement and Topics in Root Stresses of Several Gear Types", M. S. Thesis, The Ohio State University, Columbus, OH.

[25] Schmitkons, A. W., 2005. “Loaded Bevel Gear Static Transmission Error Test Stand Redesign and Assessment”, M. S. Thesis, The Ohio State University, Columbus, OH.

[26] Gosselin, C., Guertin, T., Remond, D., and Jean, Y., 2000. “Simulation and Experimental Measurement of the Transmission Error of Real Hypoid Gears Under Load”, *Journal of Mechanical Design*, **122**, 109-122